THE TRUST REGION AGGRESSIVE SPACE MAPPING
TECHNIQUE: THEORY, IMPLEMENTATION
AND EXAMPLES

M.H. Bakr, J.W. Bandler, R.M. Biernacki, S.H. Chen and K. Madsen

SOS-98-13-R

April 1998

THE TRUST REGION AGGRESSIVE SPACE MAPPING TECHNIQUE: THEORY, IMPLEMENTATION AND EXAMPLES

M.H. Bakr, J.W. Bandler, R.M. Biernacki, S.H. Chen and K. Madsen

Simulation Optimization Systems Research Laboratory
and Department of Electrical and Computer Engineering
McMaster University, Hamilton, Canada L8S 4L7

Abstract

A robust new algorithm for EM optimization of microwave circuits is presented. The algorithm integrates a trust region methodology with the aggressive space mapping (ASM). The trust region ensures that each iteration results in improved alignment between the coarse and fine models needed to execute ASM. The parameter extraction step is a crucial part of the ASM technique. The nonuniqueness of this step may result in the divergence of the technique. To improve the uniqueness of the extraction phase we developed a recursive multi-point parameter extraction. This suggested step exploits all the available electromagnetic (EM) simulations for improving the uniqueness of parameter extraction. The new algorithm was successfully used to design a number of microwave circuits. Examples include the EM optimization of a double-folded stub filter and of an HTS filter using Sonnet's *em*. The proposed algorithm was also used to design two-section, three-section and seven-section waveguide transformers exploiting Maxwell Eminence. The design of a three-section waveguide transformer with rounded corners was carried out using HP HFSS. We show how the mapping can be used to carry out Monte Carlo analysis using only coarse model simulations.

I. INTRODUCTION

A novel algorithm for aggressive space mapping (ASM) optimization [1] is introduced. Space mapping aims at aligning two different simulation models: a "coarse" model, typically an empirical circuit simulation and a "fine" model, typically a full wave EM simulation. The technique combines the accuracy of the fine model with the speed of the coarse model. Parameter extraction is a crucial part of the technique. In this step the parameters of the coarse model whose responses match the fine model responses are obtained. The extracted parameters may not be unique, causing the technique to fail to converge.

Recently, a multi-point parameter extraction concept was proposed [2] to enhance the uniqueness of the extraction step at the expense of an increased number of fine model simulations. The selection of points was arbitrary, not automated and no information about the mapping between the two spaces was taken into account.

Our proposed ASM algorithm automates the selection of fine model points used for the multi-point parameter extraction process. In the multi-point parameter extraction, an iterative approach utilizes all the fine model points simulated since the last successful iteration. Also, the current approximation to the mapping between the two spaces is integrated into the parameter extraction step. The space mapping step at each iteration is constrained by a suitable trust region [3].

The new algorithm was applied to a number of examples. The EM solver *em* [4] was used successfully to optimize the design of an HTS filter and a double-folded stub filter. Maxwell Eminence [5] through Empipe3D [6] was used as a fine model to design two-section, three-section and seven-sections waveguide transformers. HP HFSS [7] was used to carry out the optimization of a three-section waveguide transformer with rounded corners. The coarse models for these examples exploited either a coarse grid EM model or circuit-theoretic/analytical models. The different types of models used illustrate the flexibility of selection of coarse and fine models.

The required number of fine model simulations to obtain the final design, as demonstrated by the examples, is of the order of the problem dimension. Such designs would otherwise be obtained by computationally very expensive direct optimizations of the fine models.

The algorithm also establishes a mapping between the two spaces, the fine model space and the coarse model space. This mapping is updated at each iteration of the algorithm. The final mapping can be used to carry out a space-mapped Monte Carlo analysis of the fine model exploiting only coarse model simulations. We demonstrate this approach by performing a statistical analysis of the three-section waveguide transformer with rounded corners simulated by HP HFSS.

II. THE AGGRESSIVE SPACE MAPPING TECHNIQUE

It is assumed that the circuit under consideration can be simulated using two models: a fine model and a coarse model. The fine model is accurate but is computationally intensive. This model can, for example, be a finite element model. We refer to the vector of parameters of this model as x_{em}. The coarse model is a fast model but it is less accurate than the fine model. This model can be a circuit-theoretic empirical model. The vector of parameters of this model is referred to as x_{os}.

The first step of the technique is to obtain the optimal design of the coarse model x_{os}^{*}. The technique aims at establishing a mapping P between the two spaces [1]

$$x_{os} = P(x_{em}) \tag{1}$$

such that

$$\left\| R_{em}(x_{em}) - R_{os}(x_{os}) \right\| \leq \varepsilon \tag{2}$$

where R_{em} is the vector of fine model responses, R_{os} is the vector of coarse mode responses and $\left\| \; \right\|$ is a suitable norm. The error function

$$f = P(x_{em}) - x_{os}^{*} \tag{3}$$

3

is first defined. The final fine model design is obtained and the mapping is established if a solution for the system of nonlinear equations

$$f(x_{em}) = 0 \tag{4}$$

is found.

Let $x_{em}^{(i)}$ be the ith iterate in the solution of (4). The next iterate $x_{em}^{(i+1)}$ is found by a quasi-Newton iteration

$$x_{em}^{(i+1)} = x_{em}^{(i)} + h^{(i)} \tag{5}$$

where $h^{(i)}$ is obtained from

$$B^{(i)} h^{(i)} = -f(x_{em}^{(i)}) \tag{6}$$

and $B^{(i)}$ is an approximation to the Jacobian of the vector f with respect to x_{em} at the ith iteration. The matrix B is updated at each iteration using Broyden's update [8].

It is clear from (1)-(3) that the vector function f is obtained by evaluating $P(x_{em})$. This can be achieved through the process of parameter extraction. This extraction step involves solving a subsidiary optimization problem. The parameter extraction step is discussed in more detail in Section III.

III. THE PARAMETER EXTRACTION STEP

In the parameter extraction step the parameters of the coarse model whose response matches the fine model response are obtained. It can be formulated as

$$\underset{x_{os}}{minimize} \left\| R_{em}(x_{em}^{(i)}) - R_{os}(x_{os}) \right\|. \tag{7}$$

The extracted parameters may not be unique, causing the technique to fail to converge.

A multi-point parameter extraction concept was proposed [2] to enhance the uniqueness of parameter extraction at the expense of an increased number of fine model simulations. This extraction step is given by

$$minimize_{\boldsymbol{x}_{os}} \ \left\| \boldsymbol{R}_{os}(\boldsymbol{x}_{os} + \Delta \boldsymbol{x}) - \boldsymbol{R}_{em}(\boldsymbol{x}_{em} + \Delta \boldsymbol{x}) \right\|, \tag{8}$$

simultaneously for a set of perturbations $\Delta \boldsymbol{x}$. Thus the two models are matched at a number of points. In [2], there were no guidelines regarding the selection as well as the number of points used for the multi-point parameter extraction. Also, there is one important drawback in the multi-point parameter extraction procedure suggested in [2]. It was assumed that the perturbation $\Delta \boldsymbol{x}$ is identical in both spaces. This is not reliable since the relation between the perturbations in the two spaces is determined by the matrix $\boldsymbol{B}$, which is an approximation of the Jacobian of the coarse model parameters with respect to the fine model parameters, not by the identity matrix. Our new algorithm, automates the selection of fine model points used for the multi-point parameter extraction. This new algorithm is presented in the next section.

IV. THE NEW ALGORITHM

At the ith iteration, the residual vector $\boldsymbol{f}^{(i)} = \boldsymbol{P}(\boldsymbol{x}_{em}^{(i)}) - \boldsymbol{x}_{os}^{*}$ defines the difference between the vector of extracted coarse model parameters $\boldsymbol{x}_{os}^{(i)} = \boldsymbol{P}(\boldsymbol{x}_{em}^{(i)})$ and the optimal coarse model design. The mapping between the two models is established if this residual vector is driven to zero. It follows that the value $\left\| \boldsymbol{f}^{(i)} \right\|$ can serve as a measure of the misalignment between the two spaces in the ith iteration. The step taken in the ith iteration is obtained from

$$(\boldsymbol{B}^{(i)T} \boldsymbol{B}^{(i)} + \lambda \boldsymbol{I}) \boldsymbol{h}^{(i)} = -\boldsymbol{B}^{(i)T} \boldsymbol{f}^{(i)} \tag{9}$$

where $\boldsymbol{B}^{(i)}$ is an approximation to the Jacobian of the coarse model parameters with respect to the fine model parameters at the ith iteration. The parameter λ is selected such that the step obtained satisfies $\left\| \boldsymbol{h}^{(i)} \right\| \leq \delta$, where δ is the size of the trust region. This is done utilizing the iterative algorithm suggested in [3]. The point suggested for the next iteration is $\boldsymbol{x}_{em}^{(i+1)} = \boldsymbol{x}_{em}^{(i)} + \boldsymbol{h}^{(i)}$. Single point parameter extraction is then applied at the point $\boldsymbol{x}_{em}^{(i+1)}$ to get $\boldsymbol{f}_{1}^{(i+1)} = \boldsymbol{P}(\boldsymbol{x}_{em}^{(i+1)}) - \boldsymbol{x}_{os}^{*}$. The subscript of the vector $\boldsymbol{f}$ is used to

5

denote the number of points used in the parameter extraction. The absence of a subscript is used to denote a trusted value for that vector. The point $x_{em}^{(i+1)}$ is accepted and the matrix $B^{(i)}$ is updated using Broyden's formula [8] if a success criterion related to the reduction in the ℓ_2 norm of the vector f is satisfied. In our implementation, this success criterion is given by

$$\left(\left\| f^{(i)} \right\| - \left\| f_k^{(i+1)} \right\| \right) > 0.01 \left(\left\| f^{(i)} \right\| - \left\| f^{(i)} + B^{(i)} h^{(i)} \right\| \right). \tag{10}$$

The success criterion (10) ensures that the ratio between the actual reduction in the ℓ_2 norm of the vector f and the predicted reduction is greater than a certain value. Otherwise, the validity of the extraction process leading to $f_k^{(i+1)}$ at the suggested point $x_{em}^{(i+1)}$ is suspect. The residual vector $f_k^{(i+1)}$ is then used to construct a candidate point from the point $x_{em}^{(i+1)}$ by using (9). This candidate point is then added to the set of points employed for simultaneous parameter extraction at the point $x_{em}^{(i+1)}$: a new value for $f_{k+1}^{(i+1)}$ is obtained by solving

$$\underset{x_{os}}{minimize} \ \left\| R_{os}(x_{os} + B^{(i)}(x_{em} - x_{em}^{(i+1)}) - R_{em}(x_{em}) \right\|, \tag{11}$$

simultaneously for all $x_{em} \in V$, where V is the set of fine model points used for multi-point parameter extraction. This multi-point parameter extraction step differs from (8) in one important aspect. A perturbation in the fine model space of Δx_{em} corresponds to a perturbation in the coarse model space of $B^{(i)} \Delta x_{em}$. This is logical since the matrix $B^{(i)}$ represents the most up-to-date approximation to the mapping between the two spaces. Thus, the available information about the mapping between the two spaces is exploited.

The new extracted coarse model parameters either satisfy the success criterion (10) or they are used to obtain another candidate point which is then added to the set V and the whole process is repeated. See Fig. 1. This recursive multi-point parameter extraction process is expected to improve the uniqueness of the extraction step. This may lead to the satisfaction of the success criterion (10) or the step is declared a failure. Failure is declared in one of two cases: either the vector of extracted

parameters approaches a limiting value with the success criterion not satisfied, or the number of fine model simulations since the last successful iteration has reached $n+1$. In the first case, the extracted coarse model parameters are trusted and the accuracy of the linearization used to predict $\boldsymbol{h}^{(i)}$ is suspected. Thus, to ensure a successful step from the current point $\boldsymbol{x}_{em}^{(i)}$, the trust region size is shrunk and a new suggested point $\boldsymbol{x}_{em}^{(i+1)}$ is obtained. In the latter case, sufficient information is available to obtain an estimate for the Jacobian of the fine model responses with respect to the fine model parameters. This is done by solving the system of linear equations

$$
\begin{pmatrix}
(\boldsymbol{x}_{em}^{(i)}-\boldsymbol{x}_{em}^{(i+1)})^{T} \\
(\boldsymbol{x}_{em}^{(i)}-\boldsymbol{x}_{t}^{(1)})^{T} \\
\vdots \\
(\boldsymbol{x}_{em}^{(i)}-\boldsymbol{x}_{t}^{(n-1)})^{T}
\end{pmatrix}
\boldsymbol{J}^{T} =
\begin{pmatrix}
(\boldsymbol{g}^{(i)}-\boldsymbol{g}^{(i+1)})^{T} \\
(\boldsymbol{g}^{(i)}-\boldsymbol{g}_{t}^{(1)})^{T} \\
\vdots \\
(\boldsymbol{g}^{(i)}-\boldsymbol{g}_{t}^{(n-1)})^{T}
\end{pmatrix},
\tag{12}
$$

where $\boldsymbol{x}_{t}^{(k)}$ is the kth candidate point used for multi-point parameter extraction and $\boldsymbol{g}_{t}^{(k)}$ is the corresponding error between the fine model response and the optimal coarse model response. This matrix is then used to obtain a step $\boldsymbol{h}^{(i)}$ in the parameter space by solving the system of equations

$$
(\boldsymbol{J}^{T}\boldsymbol{J} + \lambda \boldsymbol{I})\boldsymbol{h}^{(i)} = -\boldsymbol{J}^{T}\boldsymbol{g}^{(i)},
\tag{13}
$$

varying the parameter λ until $\left\|\boldsymbol{h}^{(i)}\right\| \leq \delta$. If there is no reduction in the ℓ_2 norm of the vector function $\boldsymbol{g}$, the trust region is shrunk and (13) is resolved. This is repeated until either the size of the trust region has shrunk significantly and hence the algorithm terminates or a successful step is taken. The successful step is then used instead of the step obtained by (9).

At the end of each iteration, the ratio between the actual reduction in the ℓ_2 norm of the vector $\boldsymbol{f}$ and the predicted reduction using linearization is used to check the accuracy of the linearization. The criterion

$$
\left(\left\|\boldsymbol{f}^{(i)}\right\| - \left\|\boldsymbol{f}^{(i+1)}\right\|\right) \geq 0.80 \left(\left\|\boldsymbol{f}^{(i)}\right\| - \left\|\boldsymbol{f}^{(i)} + \boldsymbol{B}^{(i)}\boldsymbol{h}^{(i)}\right\|\right)
\tag{14}
$$

was used to check how accurate the linearization is. If (14) is satisfied then we exploit the accuracy of the linearization and increase the size of the trust region.

In the initialization phase we assign $x_{em}^{(0)} = x_{os}^*$ and $B^{(0)} = I$, the identity matrix. Also, we assign values to the two parameters δ_f and ε. These two parameters are used to determine the termination condition of the algorithm

As there is no iteration prior to the first iteration we are not able to compare the norm of f with a previous value to ensure the uniqueness of the step. To ensure the uniqueness of $f^{(0)}$, the multi-point parameter extraction at the first point is repeated for an increasing number of points in the set V until it approaches a limiting value. This limiting value can then be trusted and the algorithm proceeds. For any iteration $i \geq 0$, the basic steps taken are as follows.

Algorithm

Step 0   Given $x_{em}^{(i)}$, $f^{(i)}$, $B^{(i)}$ and $\delta^{(i)}$. Set $\delta^{(i+1)} = \delta^{(i)}$.

Step 1   Obtain $h^{(i)}$ by solving (9) with $\delta = \delta^{(i+1)}$. Let $\delta^{(i+1)} = \left\| h^{(i)} \right\|_2$.

Step 2   If $\delta^{(i+1)} \leq \delta_f$ stop else evaluate $x_{em}^{(i+1)}$ using (5) , set $V = \{x_{em}^{(i+1)}\}$ and $k = 1$.

Comment k is the number points used for parameter extraction.

Step 3   Apply multi-point parameter extraction using the points in the set V to obtain $f_k^{(i+1)}$.

Step 4   If the success criterion (10) is satisfied go to Step 9.

Step 5   If k is equal to one go to Step 8.

Step 6   If $\left\| f_k^{(i+1)} - f_{(k-1)}^{(i+1)} \right\| \leq \varepsilon_f$ shrink the trust region size $\delta^{(i+1)}$ and go to Step 1.

Step 7   If k is equal to n obtain an approximation for the Jacobian of the fine model responses, evaluate a new step $h^{(i)}$ by solving (13) with $\delta = \delta^{(i+1)}$ for a suitable value of λ that results in the reduction in the ℓ_2 norm of the vector g, shrink the trust region size $\delta^{(i+1)}$ and go to Step 2.

Comment The trust region is shrunk after obtaining the step $h^{(i)}$ to enable the algorithm to proceed with

a smaller trust region size if this step fails.

Step 8   Obtain a temporary point x_t^k using $x_{em}^{(i+1)}$, $f_k^{(i+1)}$ and $\delta^{(i+1)}$ by solving

$$(B^{(i)T} B^{(i)} + \lambda I) h_t^k = - B^{(i)T} f_k^{(i+1)},$$

where $\left\| h_t^k \right\| \leq \delta^{(i+1)}$ and $x_t^k = x_{em}^{(i+1)} + h_t^k$. Add this point to the set *V*, set *k=k+1*and go to Step 3.

Step 9   Set $f^{(i+1)} = f_k^{(i+1)}$ and update the matrix $B^{(i)}$ to $B^{(i+1)}$ using Broyden's formula [8].

Comment The vector $f_k^{(i+1)}$ is trusted and is used to update the matrix B.

Step 10   If $\left\| R_{em}(x_{em}^{(i+1)}) - R_{em}(x_{em}^{(i)}) \right\| \leq \varepsilon$ stop.

Step 11   Increase the trust region size $\delta^{(i+1)}$ if (14) is satisfied.

Step 12   Let *i=i+1*. Go to Step 0.

The algorithm terminates if the size of the trust region $\delta^{(i+1)}$ has shrunk below a certain

threshold or if there is no significant change in the fine model responses in two consecutive iterations.

The algorithm produces two main results. These results are the final fine model design $\bar{x}_{em}$ and the

matrix B which represents the mapping between the two spaces.

In our implementation, proper scaling is applied to the optimizable parameters to make them of

the same order. The initial trust region size is taken as 2% to 10% of the ℓ_∞ norm of the vector of

scaled parameters.

V. THE CURRENT IMPLEMENTATION

A MATLAB [9] program was written that implements the algorithm discussed in Section IV. This program requires that a settings data file be generated first. The data file is a MATLAB data file (.mat) and is used to describe the important details of the problem under consideration. It contains the following variables:

n is the number of designable parameters

m is the number of responses generated for the fine model and the coarse model. It also represents the number of responses used to match the fine model response and the coarse model response in the parameter extraction step

x_{os_opt} is the optimal coarse model design

x_{em} is the initial fine model response and is set to be equal to x_{os_opt}.

R_{os_opt} is the coarse model response corresponding to x_{os_opt}

R_{em} is the fine model response corresponding to x_{em}

B is the initial approximation to the Jacobian matrix of the coarse model parameters with respect to the fine model parameters. It is initilaized by the identity matrix.

$etta$ is a termination condition for the trust region

The first step in the MATLAB program is to load this data file to setup the problem. The algorithm then proceeds. Each time a fine model simulation is needed the MATLAB program generates a text file (simulate.dat) containing the values of the different fine model parameters. The MATLAB program then switches to the keyboard mode. This enables MATLAB to stop the execution of the algorithm until the fine model simulation is done.

In our current implementation we use OSA90/hope as a platform for obtaining the fine model responses and the results of the parameter extraction step. Two OSA90/hope input files are generated for the problem under consideration. The fine model parameters sent by MATLAB in the file (simulate.dat)

is pasted into that first file which calls the fine model simulator. The Report feature available in OSA90/hope is then used to save the fine model simulation results into a text file (simulate.m) that can be loaded into the MATLAB program. The MATLAB program then switches from the keyboard mode to the normal mode to process the received fine model responses A typical file that is used for generating the fine model responses is given in Appendix A.

The second file is used to carry out the multi-point parameter extraction. When a multi-point parameter extraction is needed, the MATLAB program generates a text file (extract.dat) containing three matrices. The first of these matrices is the matrix V of size $(n+1)$xn. Each row in this matrix corresponds to one of the points used for the parameter extraction step. The first row contains the center point of the multi-point parameter extraction. The second matrix is of dimension $(n+1)$xm. Each row of this matrix contain the fine model responses corresponding to the points in the rows of the first matrix. The third matrix represents the current approximation to the Jacobian of the coarse model parameters with respect to the fine model parameters. These three matrices are pasted into the second OSA90/hope input file. The second file then invokes the coarse model simulator and the result of the parameter extraction is saved in a text file (extract.m). This result is then loaded into the MATLAB program. A typical file used for the multi-point extraction is given in Appendix B.

V. EXAMPLES

A Two-Section 10:1 quarter wave transformer

The proposed algorithm is used for the design of a two-section 10:1 quarter wave transformer. The designable parameters for this problem are the electrical lengths of the two transmission lines at f =1.0 GHz. The design constraints for this problem are $\left| S_{11} \right| \leq 0.50$ in the frequency range $0.5 \text{ GHz} \leq f$ ≤ 1.5 GHz. The ideal transmission line model supplied by OSA90/hope [6] is used in the coarse model. Figs. 1 and 2 show the coarse model and the fine model of the filter, respectively. The fine model includes some parasitic capacitances which exist usually in practice. The values of the characteristic

11

impedances of both lines are given in Table I. The values of the parasitic capacitances are given in Table II.

The coarse model is first optimized using the minimax optimizer. It turned out that the quarter wave length is the optimal design for the coarse model for both lines. The minimax contours for the coarse model problem are shown in Fig. 3. The initial design of the fine model is taken to be the optimal design of the coarse model. The fine model responses at the starting point are shown in Fig. 4. Also, the minimax contours for the fine model problem are shown in Fig. 5. The number of required iterations is only two iterations. These two iterations required only four fine model simulations. Table III shows the obtained fine model design at each iteration. The optimal fine model responses are shown in Fig. 6. Also, the contours of the parameter extraction objective function for the first iteration are shown in Fig. 7 with a trace of the step. The change in the norm of the vector f for each iteration is shown in Fig.

It is clear from the contours of the parameter extraction step shown in Fig. 8 that the step is a well-behaved one. The smooth and fast convergence of this problem suggests that the mapping between the two spaces is close to the initial identity mapping. The fast convergence of the algorithm can also be noticed in Fig. 9, which shows the change in the ℓ_2 norm of the vector f for each iteration.

A Three-Section 3:1 microstrip transformer

The proposed algorithm is used to obtain an optimal design for a three-section 3:1 microstrip transformer [10], [11]. The filter is shown in Fig. 10. The design constraints for this problem are $|S_{11}| \leq 0.11$ in the frequency range $5\,\text{GHz} \leq f \leq 15\,\text{GHz}$. The designable parameters are the width and length of each microstrip section. The coarse model utilizes the ideal transmission line model supplied by OSA90/hope [6]. The fine model utilizes the microstrip and microstrip steps supplied by the same simulator.

The coarse model is first optimized using the minimax optimizer. The optimal coarse model solution is taken as the initial guess for the fine model design. The responses of the fine model at the

starting point are shown in Fig. 11. The final solution for this problem is obtained in only two iteration.

However, a total of six fine model simulations were needed. Most of these simulations were required to

shrink the trust region to the required accuracy to ensure the optimality of the final point. Table IV

shows the initial and final designs of the fine model. The optimal fine model responses are shown in Fig.

12. Fig. 13 shows the change in the ℓ_2 norm of the vector f at each iteration.

Double-folded Stub Filter

We consider the design of the double-folded stub (DFS) microstrip structure shown in Fig. 14

(Bandler *et al*. [12]). Folding the stubs reduces the filter area w.r.t. the conventional double stub

structure (Rautio [13]). The filter is characterized by five parameters : W_1 , W_2 , S, L_1 and L_2 (see Fig.

14). L_1, L_2 and S are chosen as optimization variables. W_1 and W_2 are fixed at 4.8 mil. The design

specifications are given by $|S_{21}| \geq$ -3 dB in the passband and $|S_{21}| \leq$ -30 dB in the stopband, where the

passband includes frequencies below 9.5 GHz and above 16.5 GHz and the stopband lies in the range [12

GHz, 14 GHz]. The structure is simulated by Sonnet's *em* [4] through Empipe [6]. The coarse model is

a coarse-grid *em* model with cell size 4.8 mil by 4.8 mil. The fine model is a fine-grid *em* model with

cell size 1.6 mil by 1.6 mil. Other parameters are summarized in Table V.

Fig. 15 shows the response along with the fine model *em* response evaluated using the optimal

coarse model parameters. The time needed to simulate the structure (coarse model) at a single frequency

is only 5 CPU seconds on a Sun SPARCstation 10. This includes the automatic response interpolation

carried out to accommodate off-grid geometries.

It is clear from Fig. 15 that the fine model response violates the design specifications at the

starting point. The new ASM algorithm required only two iterations to reach the final design . The

algorithm's progress is shown in Table VI. The number of fine model points needed is 5. Linear

response interpolation was enabled to simulate the off-grid fine model points. The response of the fine

model at the final design is shown in Fig. 16. The CPU time needed for the fine model is approximately

70 seconds per frequency point.

HTS Filter

   We consider optimization of a high-temperature superconducting (HTS) filter [1,14]. This filter is illustrated in Fig. 17. The specifications are $|S_{21}| \geq 0.95$ in the passband and $|S_{21}| \leq 0.05$ in the stopband, where the stopband includes frequencies below 3.967 GHz and above 4.099 GHz and the passband lies in the range [4.008 GHz, 4.058 GHz]. The design variables for this problem are L_1, L_2, L_3, S_1, S_2 and S_3. We take $L_0 = 50$ mil and $W = 7$ mil. The coarse model exploits the empirical models of microstrip lines, coupled lines and open stubs available in OSA90/hope. The fine model employs a fine-grid *em* simulation. The material and physical parameters values used in both OSA90/hope and in *em* are shown in Table VII. The coarse model is first optimized using the OSA90/hope minimax optimizer. The fine model response at the optimal coarse model design is shown in Fig. 18. The parameter extraction for this problem has several solutions. Fig. 19 shows how two of the extracted coarse model parameters changed with the number of points used for parameter extraction in the first iteration. The first point (1) is obtained using normal parameter extraction. These extracted values would have caused the original ASM technique to diverge. The new technique automatically generates a candidate point which is then used together with the original point to carry out a two-point parameter extraction and the second point (2) is obtained. To confirm that this point is the required one a third candidate point is automatically generated and the extraction is repeated using the three points to obtain the third extracted point (3). The second and third extracted points show that the extracted vector of coarse model parameters is approaching a limiting value and can thus be trusted. The coarse model responses corresponding to the three extracted points of Fig. 19 are shown in Fig. 20.

   For the remaining iterations, single point parameter extraction worked well. The fine model responses and the coarse model responses for the corresponding extracted points are shown in Fig. 21. The final fine model design was obtained in 5 iterations which required 8 fine model simulations. The final fine model design is given in Table VIII. The fine model response at this design is shown in Fig. 22. The passband ripples are shown in Fig. 23.

In the original space mapping approaches [1,14] this example required significant manual intervention to successfully complete the parameter extraction phase. Furthermore, without such intervention the previous approaches would not work.

Waveguide Transformers

Three designs, of two, three and seven-section waveguide transformers were considered. The two-section waveguide transformer is shown in Fig. 24. These examples are classical microwave circuit design problems [15]. Two different sets of models were used. The first set exploits two empirical models: an "ideal" analytical model which neglects the junction discontinuity and a more accurate "nonideal" analytical model which includes the junction discontinuity effects [15]. The second set uses the ideal analytical model of the first set as the coarse model while Maxwell Eminence [5] is used as the fine model. The designable parameters for these design problems are the height and length of each waveguide section.

The two-section transformer is optimized using the two analytical models. The optimum ideal model response is shown in Fig. 25 along with the nonideal model response at the same point. Our algorithm terminated in three iterations, requiring 5 fine model simulations. The final nonideal model design is given in Table IX. The corresponding nonideal model response is shown in Fig. 26. This example is known to have more than one minimum for the parameter extraction step [2]. However, our new algorithm converged successfully. The number of simulations needed to align the two models is smaller than that reported in [2]. The same transformer is then optimized using Maxwell Eminence and the ideal analytical model. Nine adaptive passes were allowed for Maxwell Eminence with allowable delta S set to 0.0001. The initial fine model response is shown in Fig. 27. The final design was obtained in three iterations which required five Maxwell Eminence fine model simulations. This is one half the number of fine model simulations reported in [2]. The Maxwell Eminence fine model design is shown in Table X and the corresponding fine model response is shown in Fig. 28.

The previous steps were repeated for the three-section waveguide transformer. The initial fine model response is shown in Fig. 29. Using the two analytical models the final design was obtained in four iterations which required six fine model simulations. This final design is shown in Table XI. The corresponding fine model response is indistinguishable from the optimal coarse model response as shown in Fig. 30.

The design of the three-section transformer is then repeated using Maxwell Eminence and the ideal analytical model. We allowed only five adaptive passes with the same value of allowable delta S as before. The initial Maxwell Eminence fine model response is shown in Fig. 31. The algorithm terminated in two iterations with a total number of nine fine model simulations. Most of these fine model simulations were used to shrink the trust region around the final design. The final design is shown in Table XII. The corresponding Maxwell Eminence fine model response is shown in Fig. 32.

The design of a seven-section waveguide transformer was also considered. The designable parameters for this problem are the height and length of each waveguide section. Using the two analytical models, the final design was obtained in three iterations which required six fine model simulations. The initial fine model response is shown in Fig. 33. The fine model response corresponding to the final design is almost identical to the optimal coarse model response as shown in Fig. 34. Table XIII shows the final fine model design.

Finally, the design of the seven-section transformer was carried out using Maxwell Eminence and an ideal analytical model. We allowed ten refinement passes with allowable delta S of 0.001. The algorithm terminated in three iterations which required eleven Maxwell Eminence fine model simulations. The initial Maxwell Eminence response is shown in Fig. 35. The final fine model response is shown in Fig. 36. Table XIV shows the corresponding Maxwell Eminence fine model design.

A Three-section Waveguide Transformer with Rounded Corners [16]

In this example we considered the design of a three-section transformer with rounded corners. The designable parameters for this problem are the height and length of each waveguide section. The

specifications are $\left| S_{11} \right| \leq$ -30 dB for a range of frequencies extending from 9.5 GHz to 15 GHz. The fine model of this circuit exploits HP HFSS [7]. The coarse model exploits an ideal empirical model that does not take into account the rounding of the corners. One quadrant of the transformer is shown in Fig. 37. We exploited the geometrical symmetry of the problem to reduce the required CPU time of HP HFSS.

Each time a new HP HFSS simulation is requested by the algorithm a new project is created using the new values for the length and height of each section. To facilitate this process, a MATLAB [9] program was developed that converts the values of the designable parameters into the corresponding HP HFSS drawing commands with the appropriate values. This approach accelerates the generation of new HP HFSS projects and eliminates the possibility of wrong dimensions.

The initial response of the fine model at the optimal coarse model design is shown in Fig. 38. Clearly, the specifications are slightly violated at this point. Only one iteration was needed to reach the final fine model design. The required number of HP HFSS simulations is seven. The first three of these simulations were needed to trust the parameter extraction at the first point. The other fine model points were needed to contract the size of the trust region to the termination size. The final HP HFSS fine model design is given in Table XV. The corresponding fine model response is shown in Fig. 39.

VI. MONTE CARLO ANALYSIS USING SPACE MAPPING [12]

The final $\boldsymbol{B}$ matrix obtained by the algorithm represents the best available information about the mapping between the two spaces. A perturbation of $\Delta \boldsymbol{x}_{em}$ in the fine model space is mapped to a perturbation of $\Delta \boldsymbol{x}_{os}$ in the coarse model space by

$$\Delta \boldsymbol{x}_{os} = \boldsymbol{B} \Delta \boldsymbol{x}_{em} \tag{15}$$

The perturbations in the coarse model space and fine model space are with respect to $\boldsymbol{x}_{os}^{*}$ and $\overline{\boldsymbol{x}}_{em}$, respectively. The established mapping can be used to perform a space-mapped Monte Carlo analysis

[12] for the problem under consideration. The random points generated in the fine model space are mapped to the coarse model space using (15). Coarse model simulations are then used instead of the CPU intensive fine model points. This statistical analysis should enjoy the speed of the coarse model and the accuracy of the fine model.

To demonstrate this approach we carried out a Monte Carlo analysis of the three-section waveguide transformer with rounded corners. The fine model parameters were assumed to be uniformly distributed with tolerances of 1%, 2% and 5%. The corresponding responses are shown in Figs. 28, 29 and 30. The estimated yields for these tolerances are 39%, 4% and 0%.

REFERENCES

[1] J.W. Bandler, R.M. Biernacki, S.H. Chen, R.H. Hemmers and K. Madsen, "Electromagnetic optimization exploiting aggressive space mapping," *IEEE Trans. Microwave Theory Tech.*, vol. 43, 1995, pp. 2874-2882.

[2] J.W. Bandler, R.M. Biernacki and S.H. Chen, "Fully automated space mapping optimization of 3D structures," *IEEE MTT-S Int. Microwave Symp. Dig.* (San Francisco, CA), 1996, pp. 753-756.

[3] J.J. Moré and D.C. Sorenson, "Computing a trust region step," *SIAM J. Sci. Stat. Comp.*, vol. 4, 1983, pp. 553-572.

[4] *em*™ , Version 3.0a, Sonnet Software, Inc., Liverpool, NY 13088, 1996.

[5] *Maxwell Eminence*, Version 4.02, Ansoft Corporation, Four Station Square, Suite 660, Pittsburgh, PA 15219, USA.

[6] OSA90/hope™, Empipe™ and Empipe3D™, Version 4.0, Optimization Systems Associates Inc., ON, Canada, 1997.

[7] *HP HFSS*, Version 5.0, Hewlett-Packard Co., 1400 Fountaingrove Parkway, Santa Rosa, CA 95403, 1997.

[8] C.G. Broyden, "A class of methods for solving nonlinear simultaneous equations," *Math. Comp.*, vol. 19, 1965, pp. 577-593.

[9] MATLAB®, Version 5.0, The Math. Works, Inc., 24 Prime Park Way, Natick, MA 01760, 1997.

[10] J.W. Bandler, R.M. Biernacki, S.H. Chen, P.A. Grobelny and R.H. Hemmers, "Space mapping technique for electromagnetic optimiztion," *IEEE Trans. Microwave Theory Tech.,* vol. 42, 1994, pp. 2536-2544.

[11] J.W. Bandler, R.M. Biernacki, S.H. Chen, P.A. Grobelny and S. Ye, "Yield-driven electromagnetic optimization via multi-level multi-dimensional models," *IEEE Trans. Microwave Theory Tech.*, vol. 41, 1993, pp. 2269-2278.

[12] J.W. Bandler, R.M. Biernacki, S.H. Chen, P.A. Grobelny and D.G. Swanson, "Heterogeneous parallel yield-driven electromagnetic CAD," *IEEE MTT-S Int. Microwave Symp.* (Orlando, FL), 1995, pp. 1085-1088.

[13] J.C. Rautio, Sonnet Software, Inc., 1020 Seventh North Street, Suite 210, Liverpool, NY 13088, Private Communication, 1992.

[14] J.W. Bandler, R.M. Biernacki, S.H. Chen, W.J. Gestinger, P.A. Grobelny, C. Moskowitz and S.H. Talisa, "Electromagnetic design of high-temperature superconducting filters," *Int. J. Microwave and Millimeter-Wave CAE*, vol. 5, 1995, pp. 331-343.

[15] J.W. Bandler, "Computer optimization of inhomogeneous waveguide transformers," *IEEE Trans. Microwave Theory Tech.*, vol. MTT-17, 1969, pp. 563-571.

[16] *Empipe3D™ Manual*, Version 4.0, Optimization Systems Associates Inc., ON, Canada, Chapter 5, 1997.

TABLE I
THE CHARACTERISTIC IMPEDANCES OF BOTH LINES FOR
THE TWO-SECTION TRANSFORMER

Impedance	Value
Z_1	2.23615
Z_2	4.47230
all values are in ohm	

TABLE II
PARASITIC CAPACITANCES OF FINE MODEL FOR
THE TWO-SECTION TRANSFORMER

Capacitance	Value
C_1	2.5
C_2	2.5
C_3	2.5
all values are in pF	

TABLE III
FINE MODEL DESIGNS AT EACH ITERATION FOR
THE TWO-SECTION TRANSFORMER

Parameter	$x_{em}^{(0)}$	$x_{em}^{(1)}$	$x_{em}^{(2)}$
L_1	90.0000	88.25264	88.19323
L_2	90.0000	88.99598	88.93862
all values are in degrees			

TABLE IV
THE INITIAL AND FINAL DESIGNS OF THE FINE MODEL FOR
THE THREE-SECTION 3:1 MICROSTRIP TRANSFORMER

Parameter	$x_{em}^{(0)}$	$x_{em}^{(2)}$
W_1	0.38100	0.38868
L_1	2.98820	2.82103
W_2	0.15240	0.15512
L_2	3.07176	2.99830
W_3	0.04480	0.04312
L_3	3.14610	3.06224
all values are in mm		

TABLE V
MATERIAL AND PHYSICAL PARAMETERS FOR THE COARSE
AND FINE *em* MODELS OF THE DFS FILTER

Model Parameter	Value
substrate dielectric constant	9.9
substrate thickness (mil)	5
shielding cover height (mil)	∞
conducting material thickness	3.0E-6
substrate dielectric loss tangent	2.0E-3
resistivity of metal (Ωm)	1.72E-8
magnetic loss tangent	0
surface reactance (Ω/sq)	0
lower frequency limit (GHz)	5
upper frequency limit (GHz)	20
frequency increment size (GHz)	0.25

TABLE VI
VALUES OF OPTIMIZABLE PARAMETERS AT EACH ITERATION
FOR THE DFS FILTER

Parameter	$x_{em}^{(0)}$	$x_{em}^{(1)}$	$x_{em}^{(2)}$
L_1	88.8	89.5	94.3
L_2	84.1	84.6	85.4
S	3.9	4.7	4.7
all values are in mils			

TABLE VII
MATERIAL AND PHYSICAL PARAMETERS FOR THE HTS FILTER

Model Parameter	OSA90/hope	*em*
substrate dielectric constant	23.425	23.425
substrate thickness (mil)	19.9516	19.9516
shielding cover height (mil)	∞	250
conducting material thickness	1.968E-2	0
substrate dielectric loss tangent	3.0E-5	3.0E-5
resistivity of metal (Ωm)	0	4.032E-8
surface roughness of metal	0	—
magnetic loss tangent	—	0
surface reactance (Ω/sq)	—	0
x-grid cell size (mil)	—	1.00
y-grid cell size (mil)	—	1.75

TABLE VIII
THE INITIAL AND FINAL DESIGNS OF THE FINE MODEL
FOR THE HTS FILTER

Parameter	$x_{em}^{(0)}$	$x_{em}^{(5)}$
L_1	188.33	181.43
L_2	197.98	200.51
L_3	188.58	180.49
S_1	21.97	19.44
S_2	99.12	80.52
S_3	111.67	83.41
all values are in mils		

TABLE IX
VALUES OF OPTIMIZABLE PARAMETERS AT EACH ITERATION OF THE NEW
ASM TECHNIQUE FOR THE TWO-SECTION WAVEGUIDE TRANSFORMER
USING TWO ANALYTICAL MODELS

Parameter	$x_{em}^{(0)}$	$x_{em}^{(1)}$	$x_{em}^{(2)}$	$x_{em}^{(3)}$
b_1	0.712	0.715	0.716	0.716
b_2	1.395	1.400	1.402	1.402
L_1	1.657	1.591	1.560	1.560
L_2	1.590	1.541	1.518	1.518
all values are in cm				

TABLE X

VALUES OF OPTIMIZABLE PARAMETERSAT EACH ITERATION OF THE NEW ASM
TECHNIQUE FOR THE TWO-SECTION WAVEGUIDE TRANSFORMER USING
MAXWELL EMINENCE AND AN IDEAL ANALYTICAL MODEL

Parameter	$x_{em}^{(0)}$	$x_{em}^{(1)}$	$x_{em}^{(2)}$	$x_{em}^{(3)}$
b_1	0.712	0.713	0.719	0.716
b_2	1.395	1.397	1.408	1.402
L_1	1.657	1.595	1.565	1.567
L_2	1.590	1.535	1.517	1.517
all values are in cm				

TABLE XI

VALUES OF OPTIMIZABLE PARAMETERS AT EACH ITERATION OF THE NEW
ASM TECHNIQUE FOR THE THREE-SECTION WAVEGUIDE
TRANSFORMER USING TWO ANALYTICAL MODELS

Parameter	$x_{em}^{(0)}$	$x_{em}^{(1)}$	$x_{em}^{(2)}$	$x_{em}^{(3)}$	$x_{em}^{(4)}$
b_1	0.903	0.905	0.881	0.891	0.892
b_2	1.371	1.363	1.298	1.325	1.325
b_3	1.736	1.718	1.692	1.701	1.702
L_1	1.549	1.500	1.500	1.489	1.489
L_2	1.584	1.575	1.575	1.575	1.577
L_3	1.646	1.768	1.880	1.853	1.850
all values are in cm					

TABLE XII
VALUES OF OPTIMIZABLE PARAMETERS AT EACH ITERATION OF THE NEW ASM
TECHNIQUE FOR THE THREE-SECTION WAVEGUIDE TRANSFORMER
USING MAXWELL EMINENCE AND AN IDEAL ANALYTICAL MODEL

Parameter	$\boldsymbol{x}_{em}^{(0)}$	$\boldsymbol{x}_{em}^{(1)}$	$\boldsymbol{x}_{em}^{(2)}$
b_1	0.903	0.898	0.893
b_2	1.371	1.340	1.327
b_3	1.736	1.707	1.703
L_1	1.549	1.514	1.495
L_2	1.584	1.566	1.568
L_3	1.646	1.810	1.848

all values are in cm

TABLE XIII
VALUES OF OPTIMIZABLE PARAMETERS AT THE INITIAL AND FINAL
DESIGN FOR THE SEVEN-SECTION WAVEGUIDE TRANSFORMER
USING TWO ANALYTICAL MODELS

Parameter	$\boldsymbol{x}_{em}^{(0)}$	$\boldsymbol{x}_{em}^{(3)}$
b_1	7.86732	7.87152
b_2	6.61888	6.64855
b_3	4.68540	4.74039
b_4	2.91987	2.96613
b_5	1.81412	1.83659
b_6	1.27658	1.28401
b_7	1.06847	1.06967
L_1	7.10588	7.24590
L_2	7.12201	7.08753
L_3	7.11760	6.91817
L_4	7.12331	6.90979
L_5	7.12815	6.98383
L_6	7.12154	7.03845
L_7	7.12945	7.07431

all values are in cm

TABLE XIV
VALUES OF OPTIMIZABLE PARAMETERS AT THE INITIAL AND FINAL DESIGN
FOR THE SEVEN-SECTION WAVEGUIDE TRANSFORMER USING
MAXWELL EMINENCE AND AN IDEAL ANALYTICAL MODEL

Parameter	$x_{em}^{(0)}$	$x_{em}^{(3)}$
b_1	7.86732	7.87494
b_2	6.61888	6.65247
b_3	4.68540	4.74347
b_4	2.91987	2.97030
b_5	1.81412	1.84134
b_6	1.27658	1.28891
b_7	1.06847	1.07201
L_1	7.10588	7.18744
L_2	7.12201	7.03537
L_3	7.11760	6.89166
L_4	7.12331	6.89697
L_5	7.12815	6.98825
L_6	7.12154	7.05869
L_7	7.12945	7.12572

all values are in cm

TABLE XV
VALUES OF OPTIMIZABLE PARAMETERS AT EACH ITERATION OF THE NEW ASM
TECHNIQUE FOR THE THREE-SECTION WAVEGUIDE TRANSFORMER WITH ROUND
CORNERS USING HPHFSS AND AN IDEAL ANALAYTICAL MODEL

Parameter	$x_{em}^{(0)}$	$x_{em}^{(1)}$
b_1	0.33276	0.32971
b_2	0.26551	0.26396
b_3	0.21186	0.20978
L_1	0.32556	0.33208
L_2	0.32640	0.32335
L_3	0.32556	0.32192

all values are in inch

the current state at the ith iteration

initial parameter extraction at the suggested point $\boldsymbol{x}_{em}^{i+1}$

parameter extraction fails; an additional point $\boldsymbol{x}_t^1$ is obtained and multi-point parameter extraction is carried out to sharpen the solution
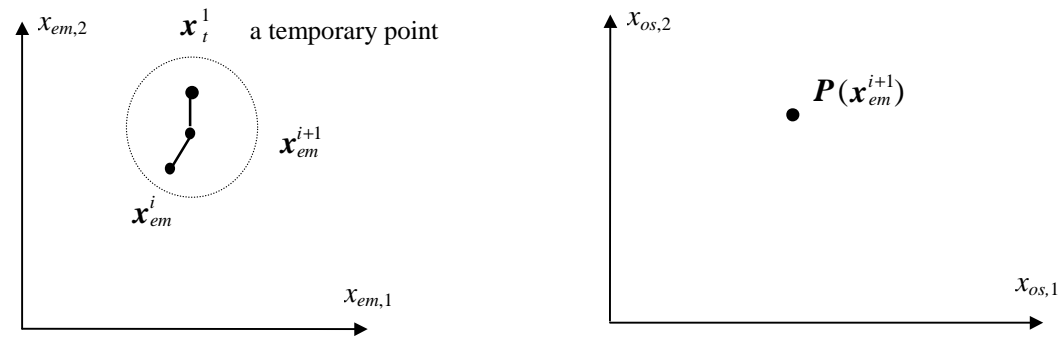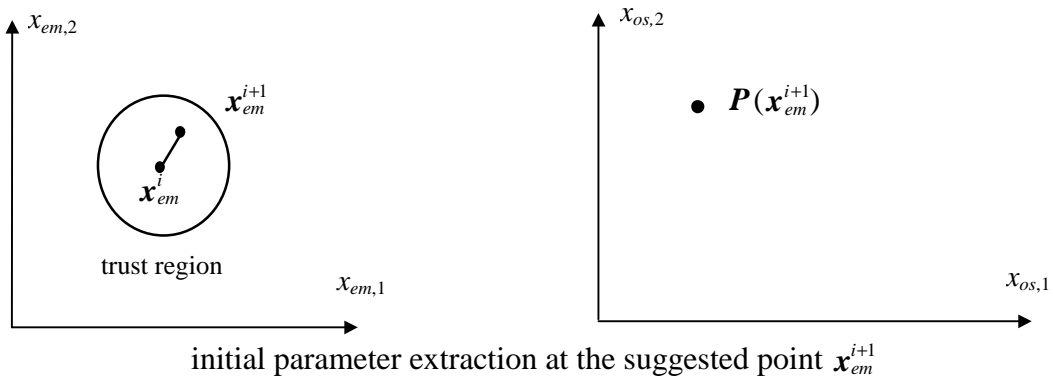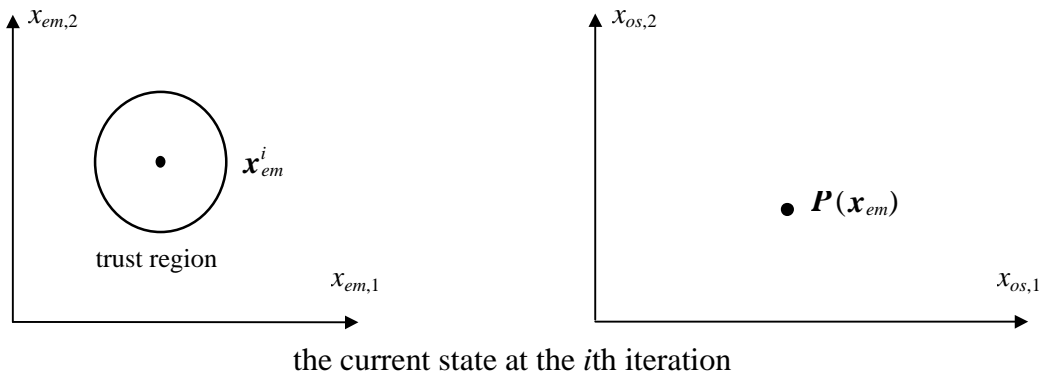
Fig. 1. Illustration of the automated multi-point parameter extraction.
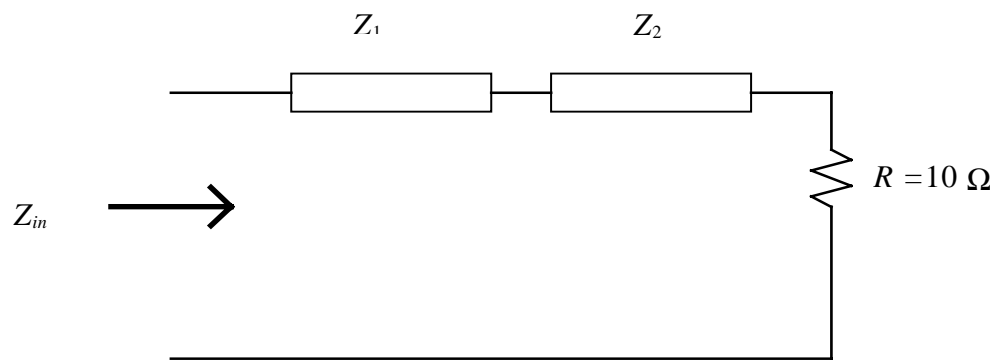
Fig. 2. The coarse model of the two-section transformer.
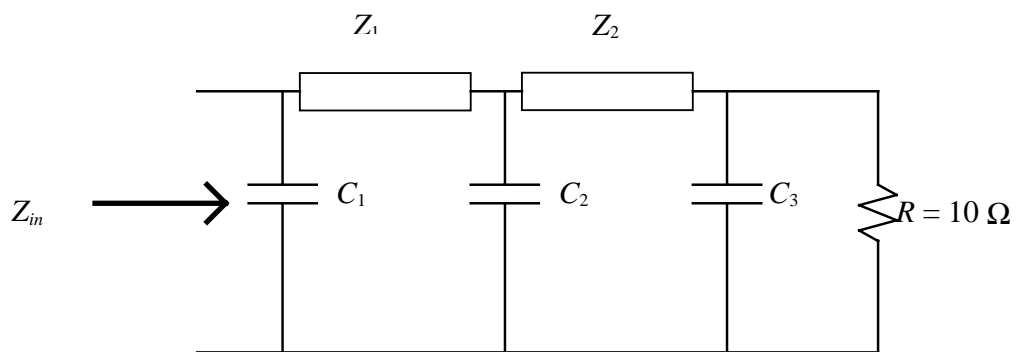
Fig. 3. The fine model of the two-section transformer.
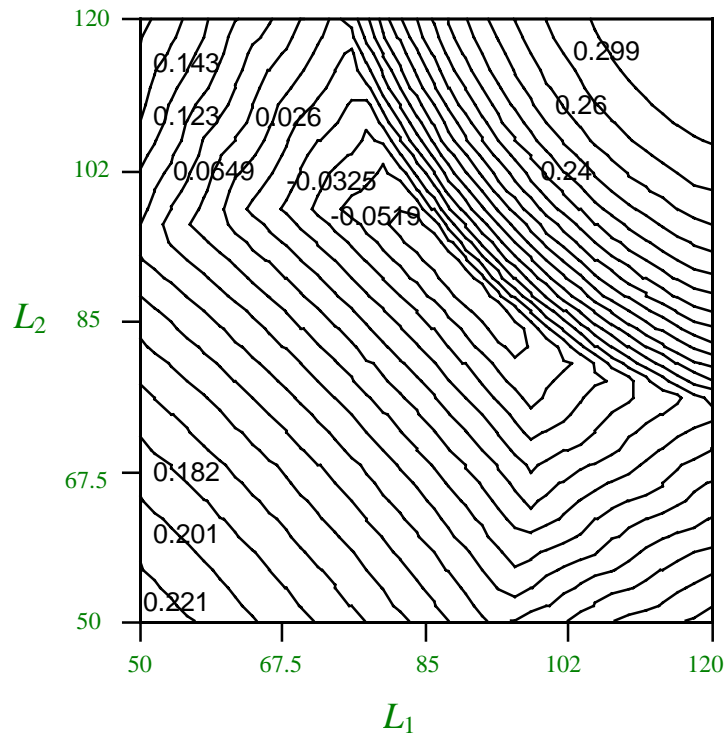
Fig. 4. The minimax contours of the coarse model problem for the two-section transformer.
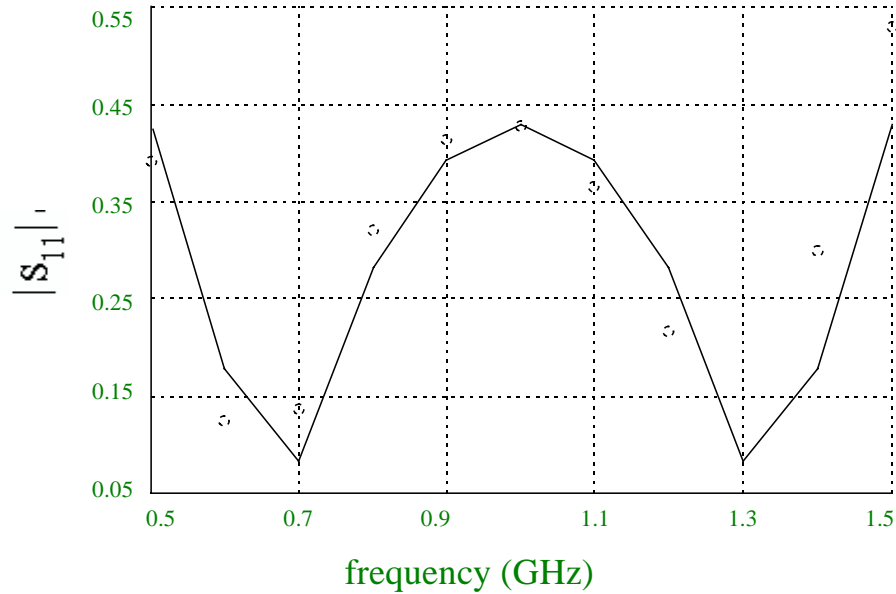
Fig. 5. The optimal coarse model response (—) and the fine model response (o)
at the starting point for the two-section transformer .

29
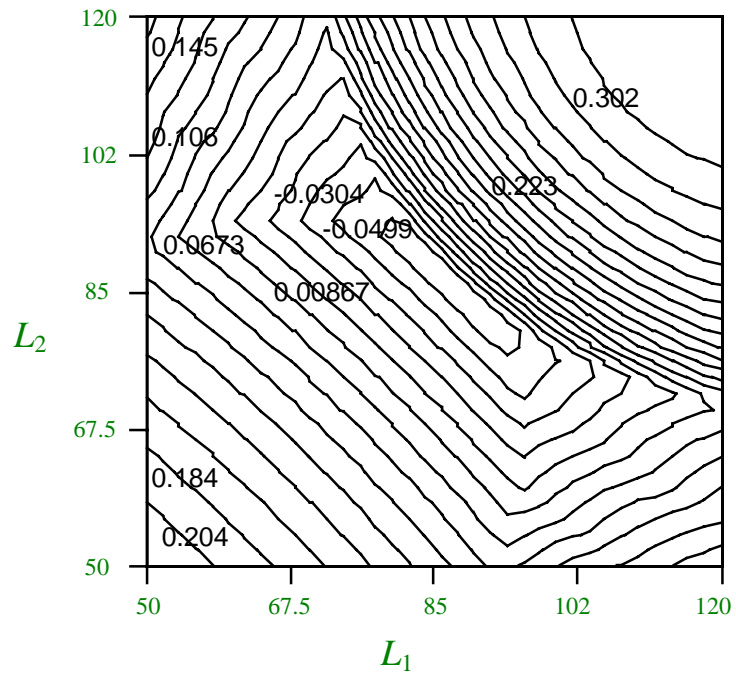
Fig. 6. The minimax contours of the fine model problem for
the two-section transformer.
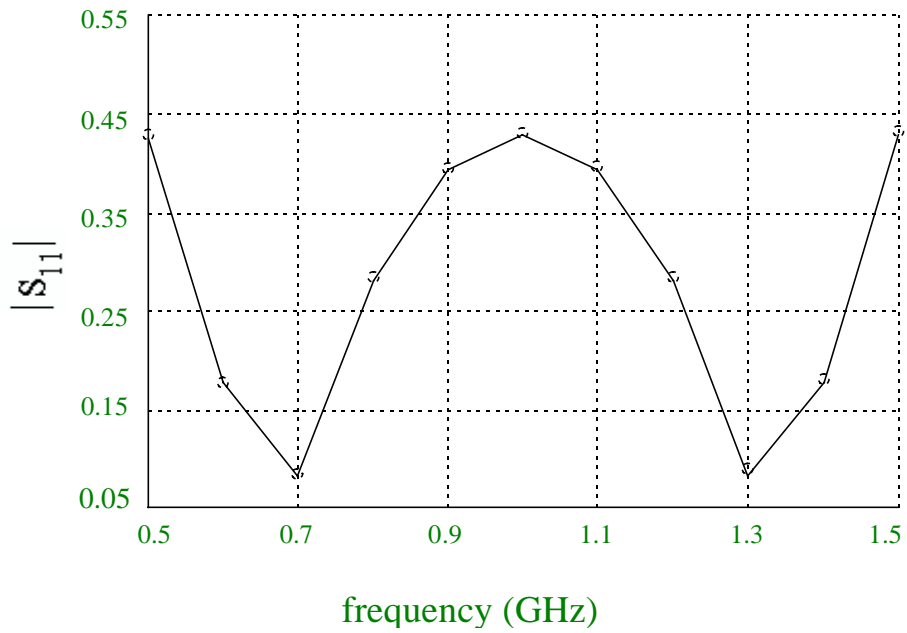
Fig. 7. The optimal coarse model response (—) and the final fine model
response (o) for the two-section transformer.
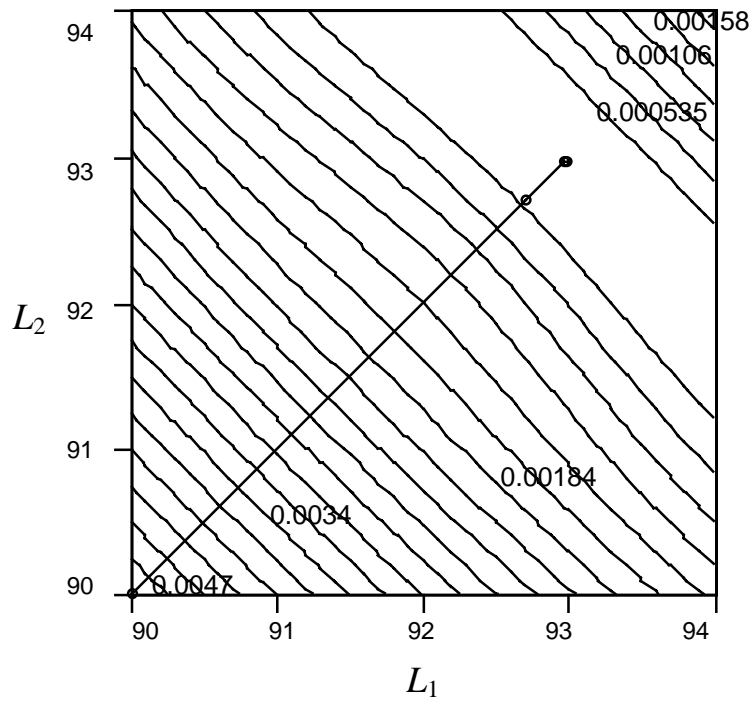
Fig. 8. The contours of the parameter extraction step for the two-section transformer at the first iteration.
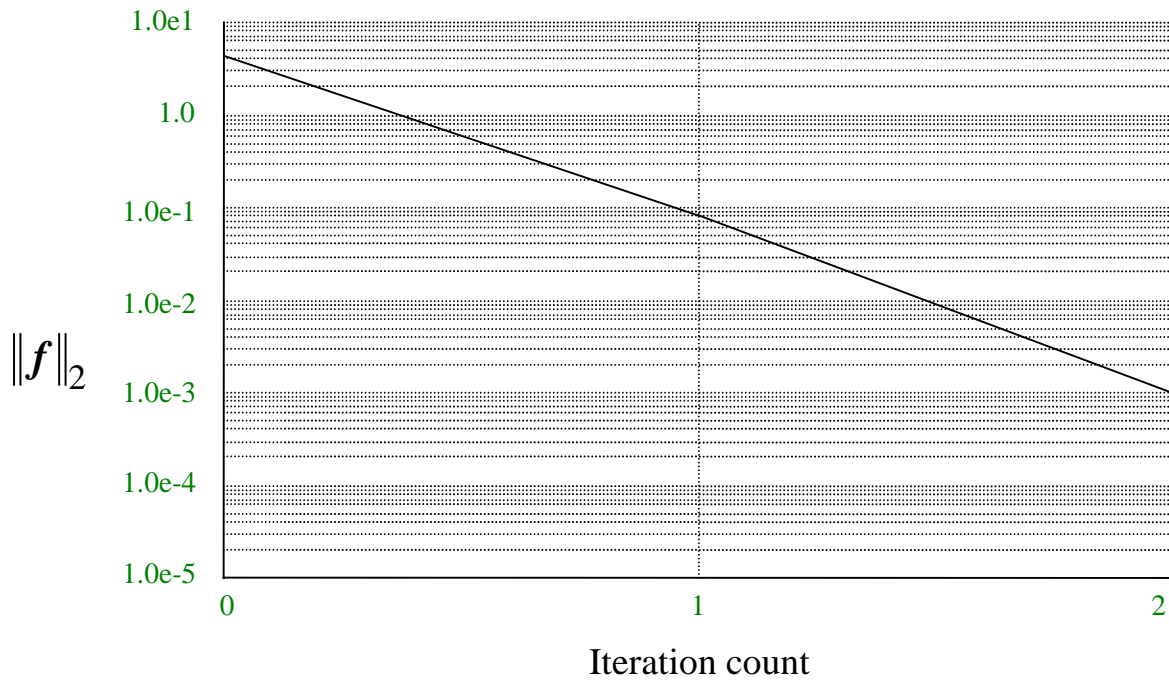
Fig. 9. The change of the ℓ_2 norm of the vector $\boldsymbol{f}$ with the number of iterations for the two-section transformer.
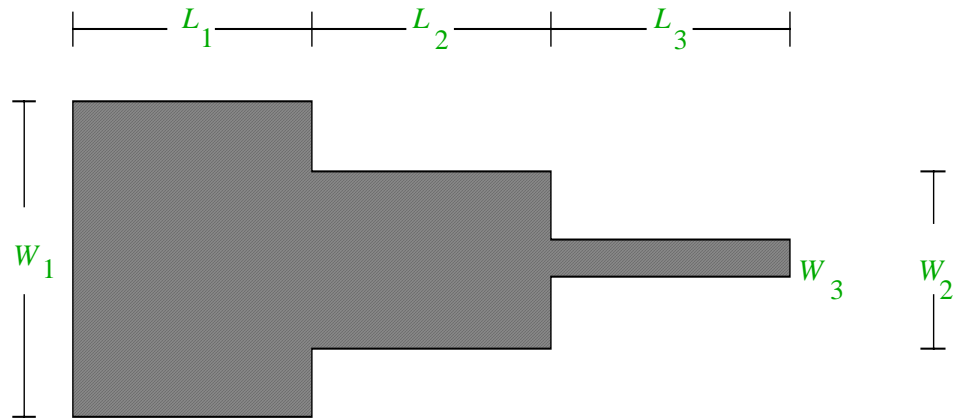
Fig. 10. The three-section 3:1 microstrip transformer.
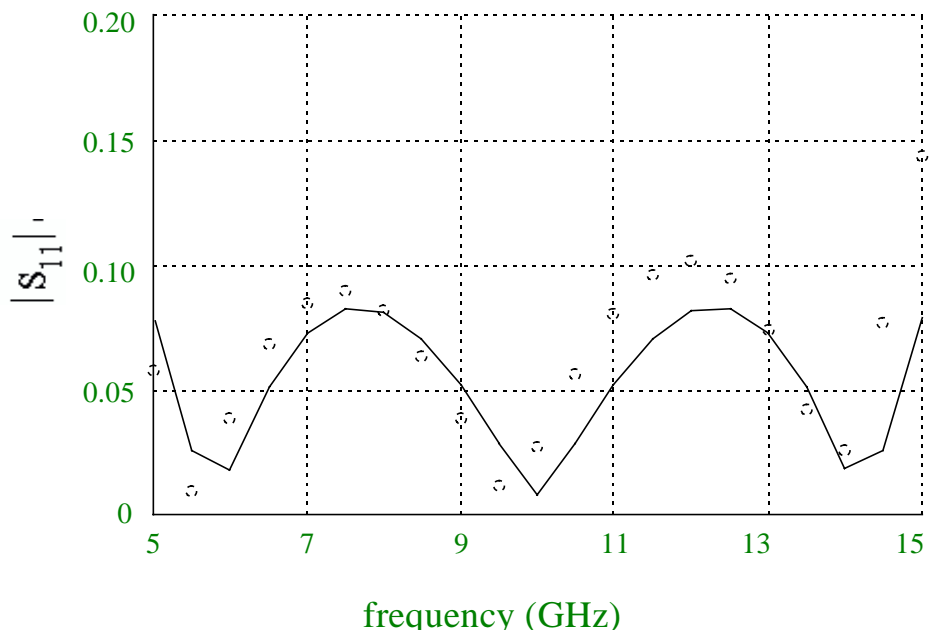
Fig. 11. The optimal coarse model response (——) and the fine model response (o) at the starting point for the three-section microstrip transformer.
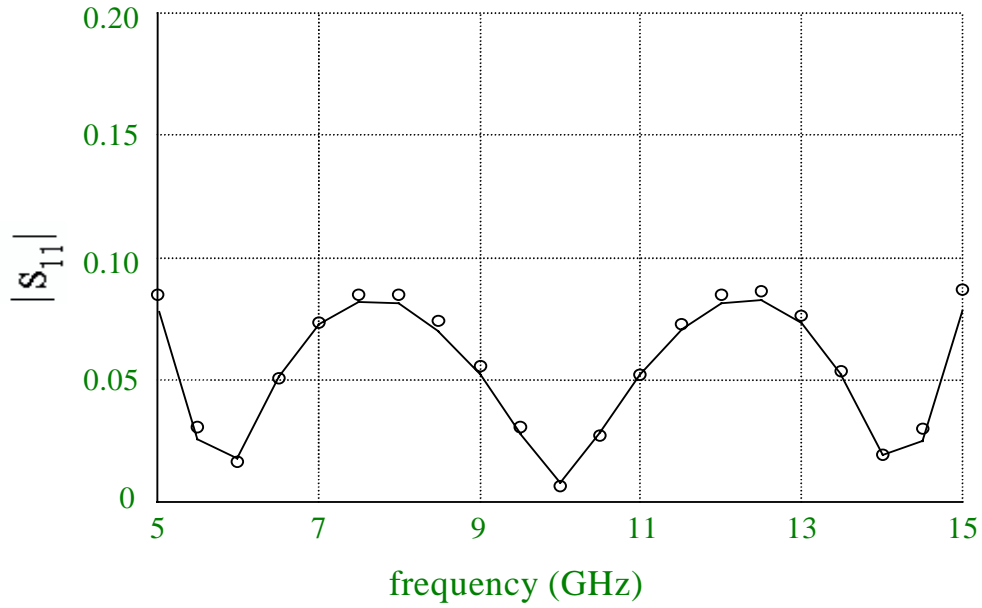
Fig. 12. The optimal coarse model response (—) and the final fine model
response (○) for the three-section microstrip transformer.
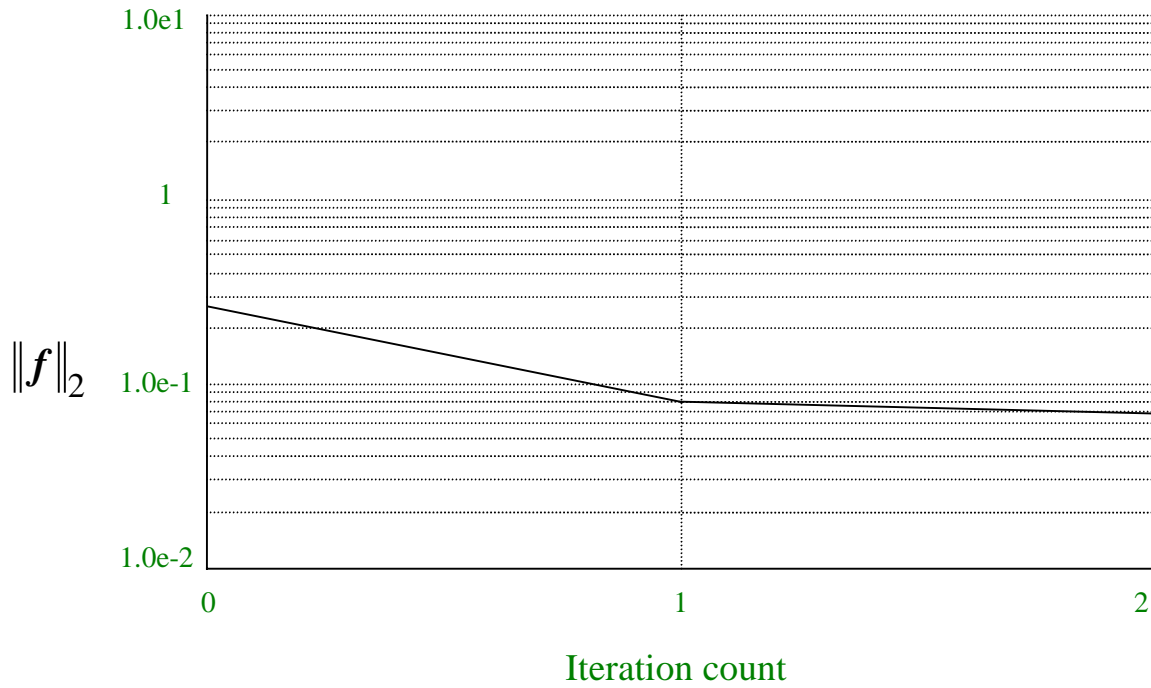
Fig. 13. The change of the ℓ_2 norm of the vector f with the number of iterations
for the three-section microstrip transformer.

33
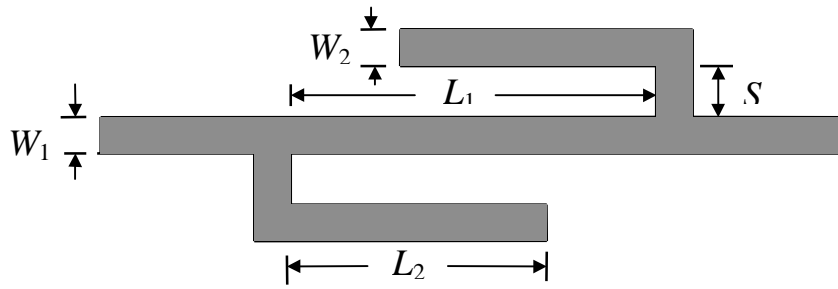
Fig. 14. The DFS filter [9].
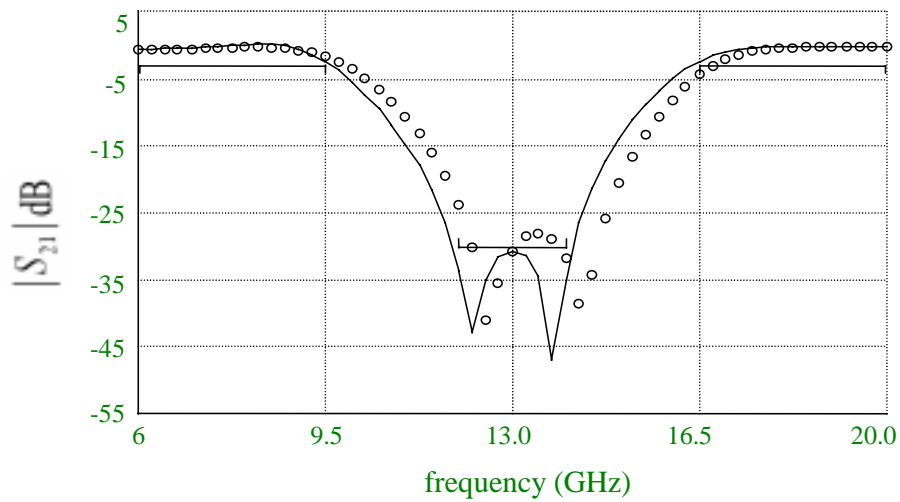
Fig. 15. The optimal coarse model response (—) and the fine model response (o)
at the starting point for the DFS filter .
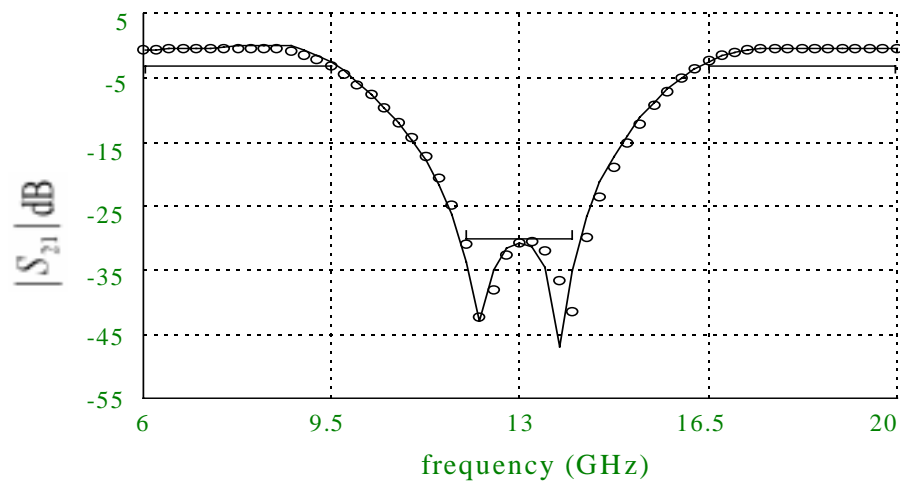
Fig. 16. The optimal coarse model response (—) and the final fine model
response (o) for the DFS filter.
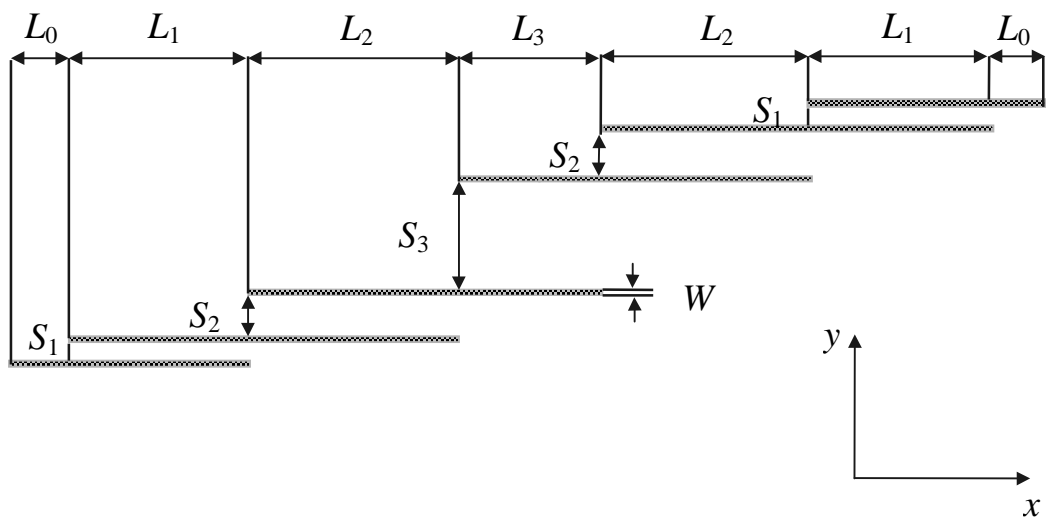
Fig. 17. The structure of the HTS filter [1,11].
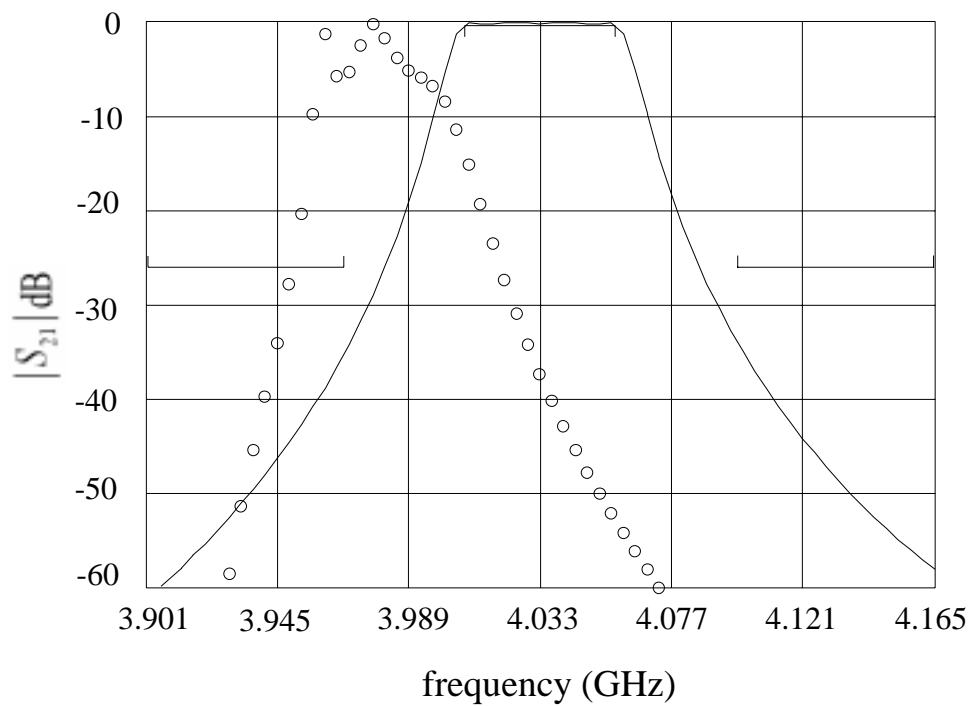
Fig. 18. The optimal coarse model response (——) and the fine model response (o) at the starting point for the HTS filter.
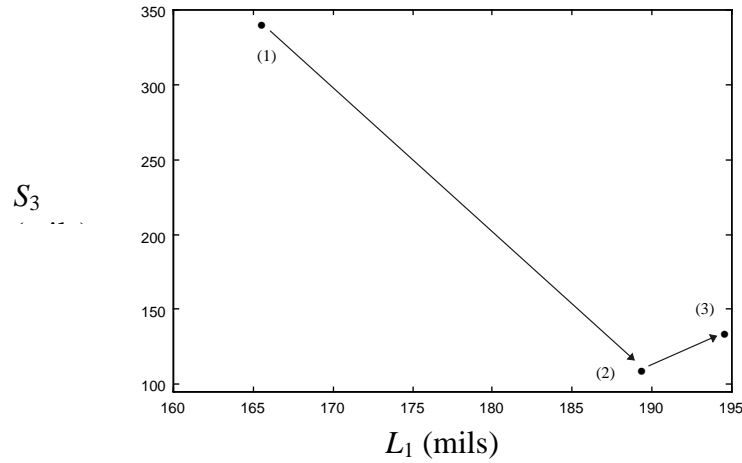
Fig. 19. The variation of two of the extracted coarse model parameters in the first iteration with the number of points used for parameter extraction where (1) is obtained using a single fine model point, (2) is obtained using two fine model points and (3) is obtained using three fine model points.

(a)

(b)

(c)
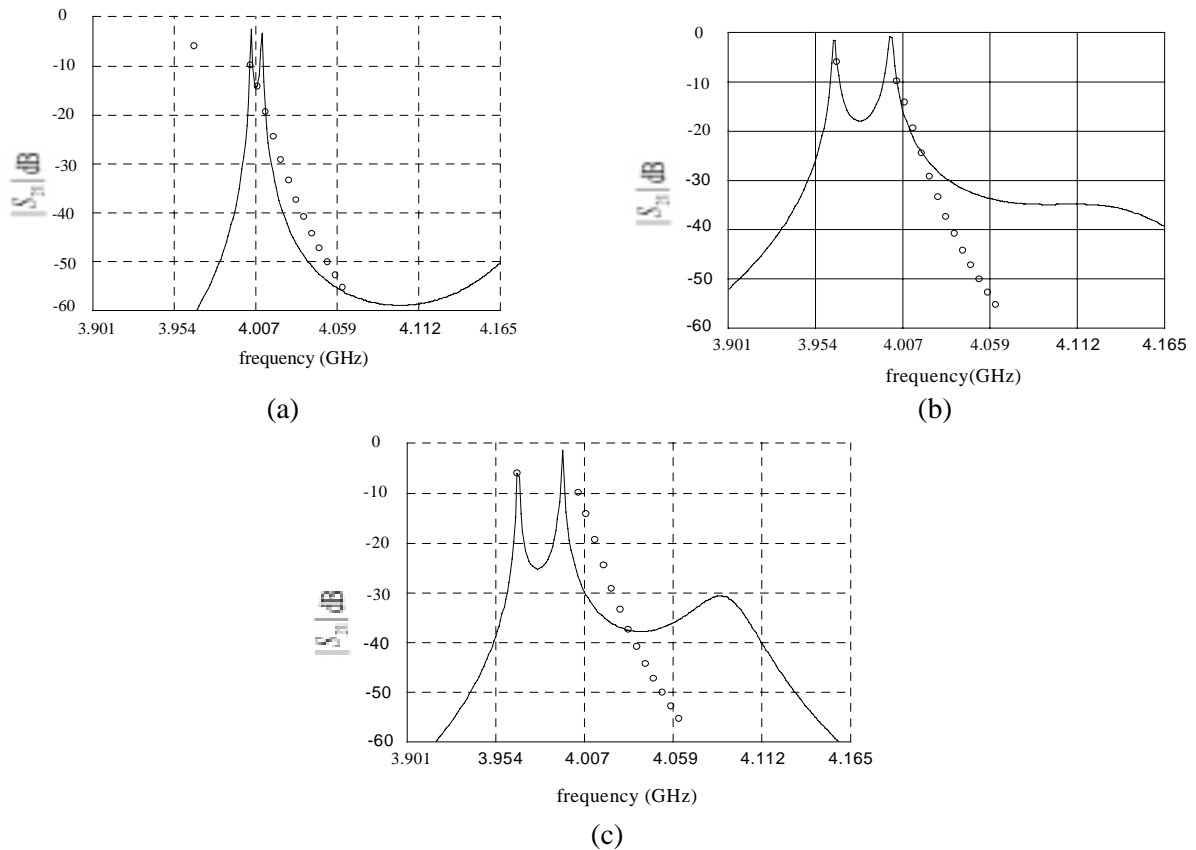
Fig. 20. The coarse model response (—) and the fine model response (o) corresponding to the three extracted points in Fig. 7 where (a) is obtained using a single fine model, (b) is obtained using two fine model points and (c) is obtained using three fine model points.
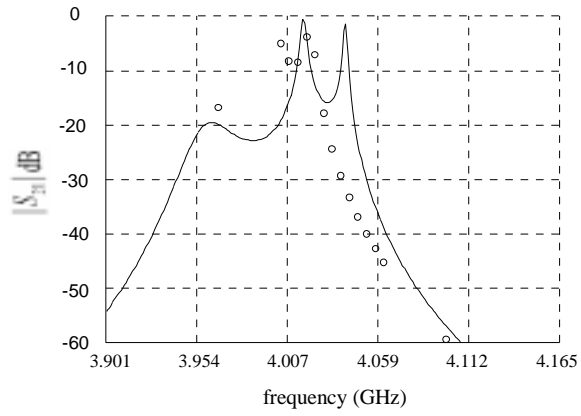
(a)
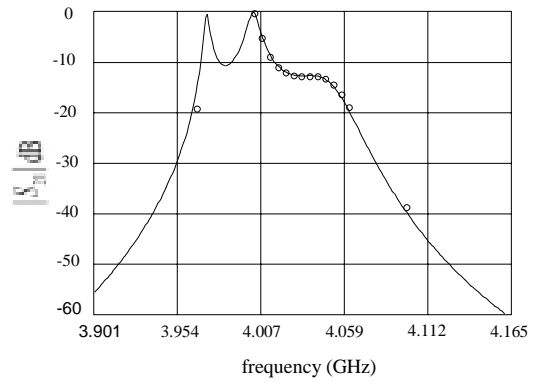
(b)
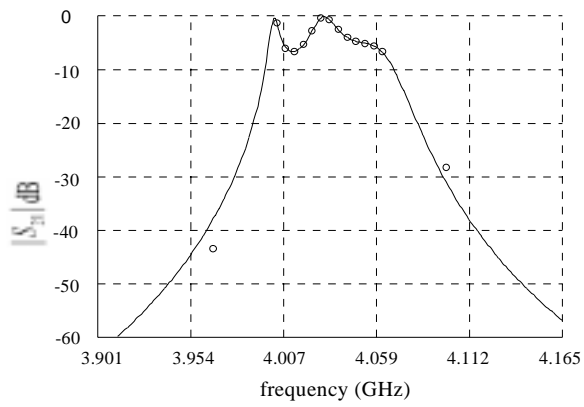
(c)
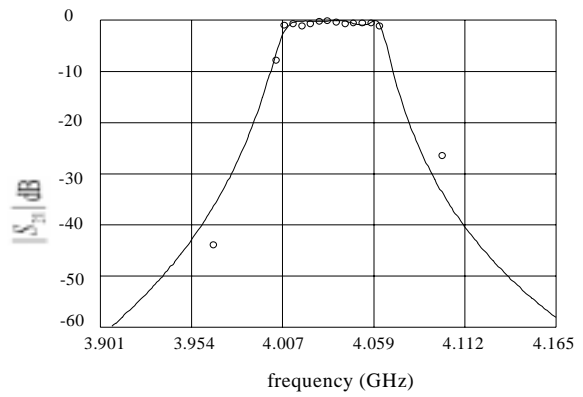
(d)

Fig. 21. The coarse model response (—) at the extracted point and the fine model response (o) corresponding to the second, third, fourth and fifth iterations.

37
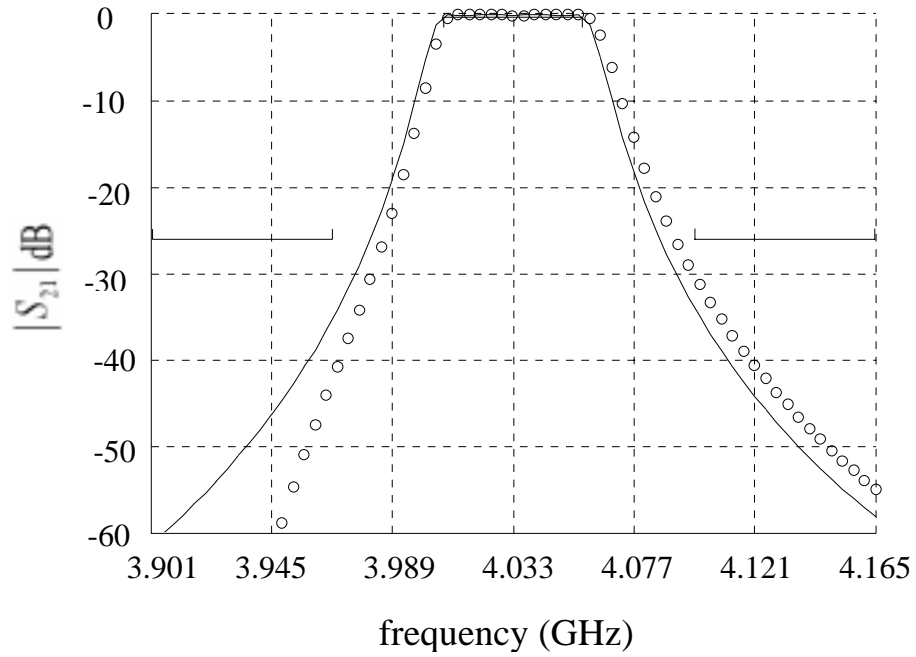
Fig. 22. The optimal coarse model response (—) and the final fine model response (o) for the HTS filter.
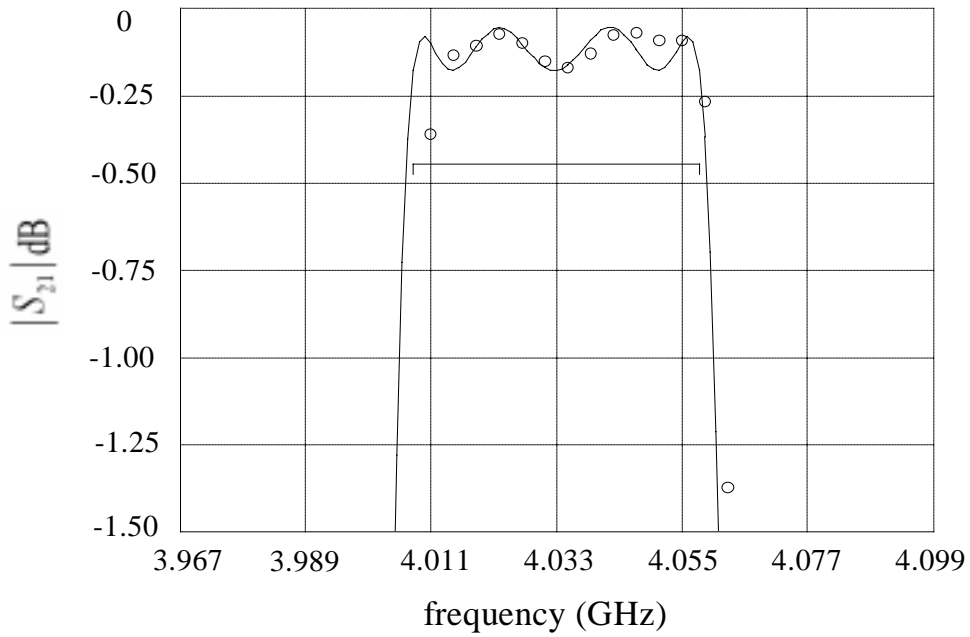
Fig. 23. The optimal coarse model response (—) and the final fine model response (o) for the HTS filter in the passband.
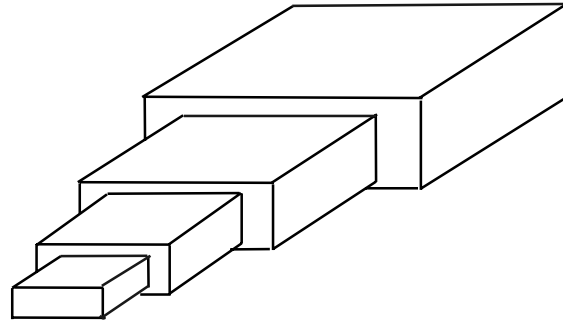
Fig. 24. A typical two-section waveguide transformer.
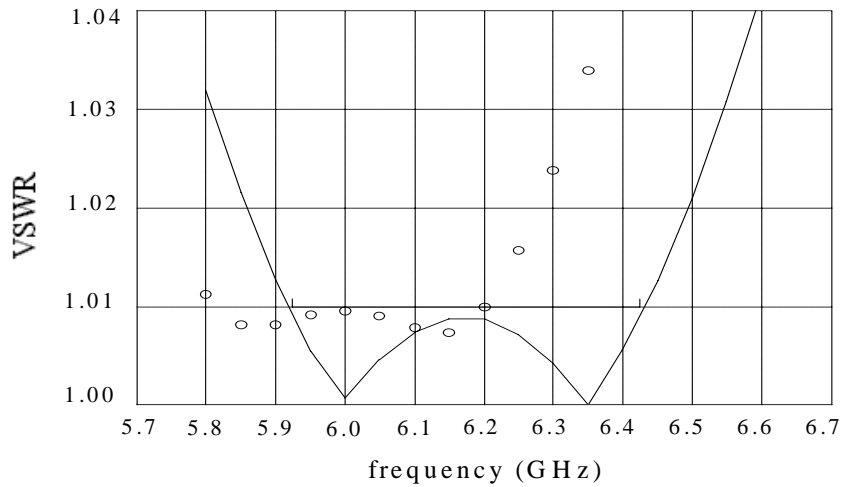
Fig. 25. The optimal response of the ideal analytical model (——) and the response of the nonideal analytical model (o) at the starting point for the two-section waveguide transformer.
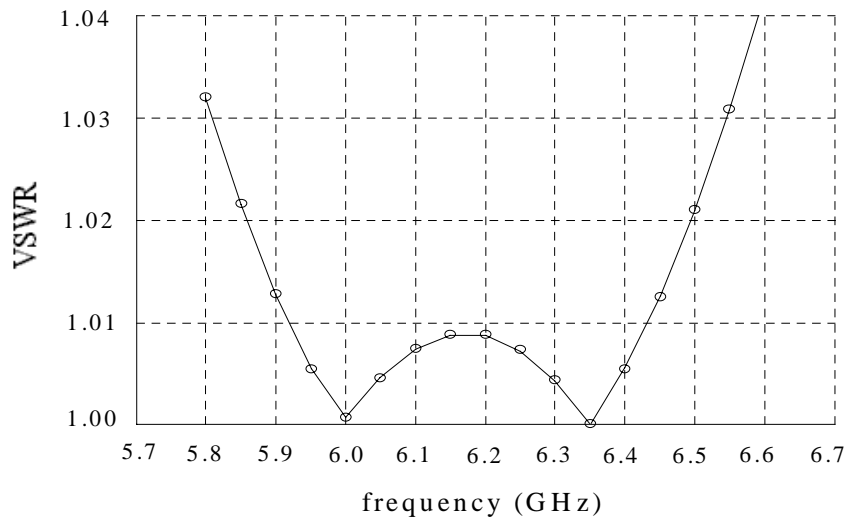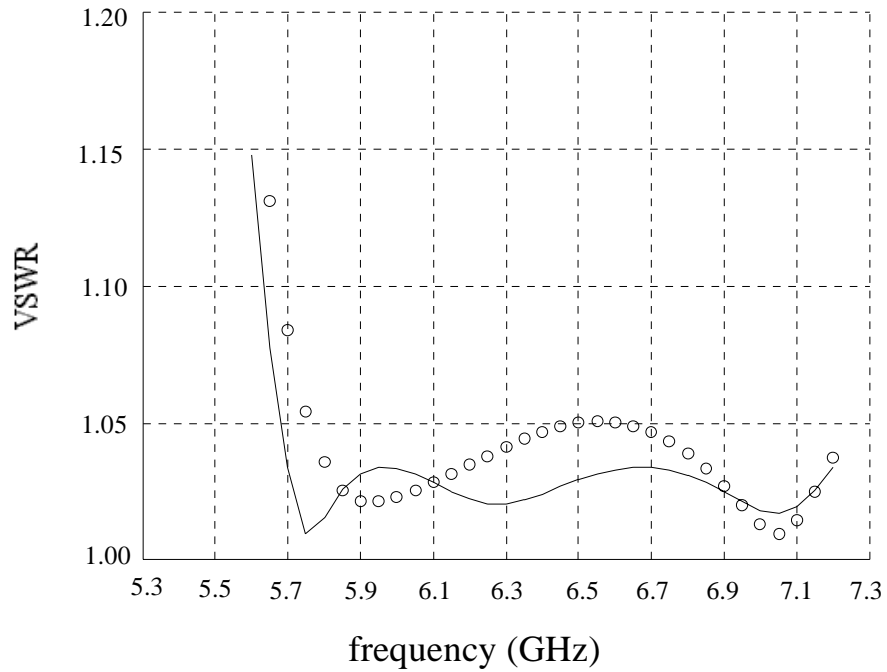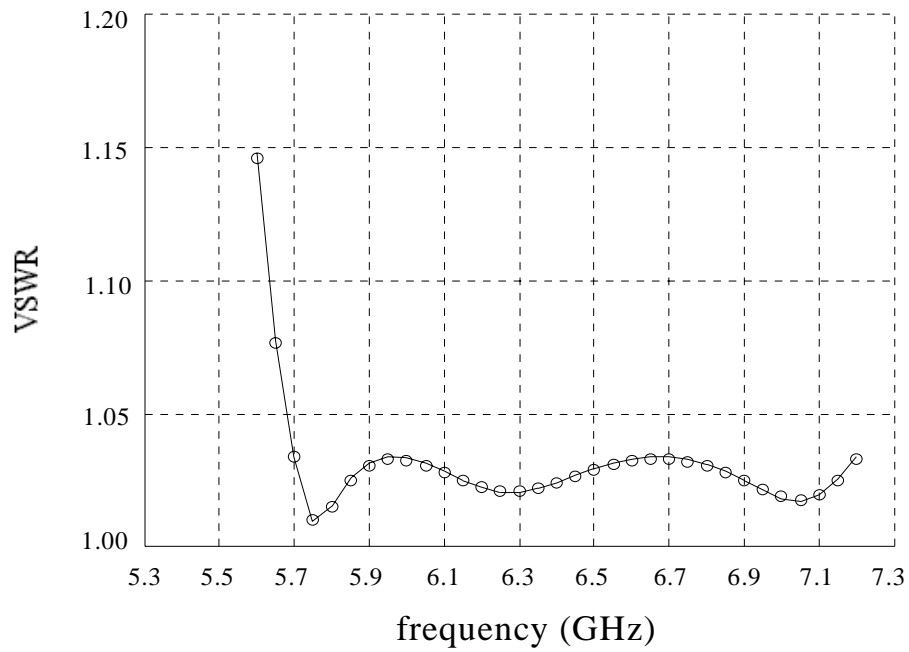

Fig. 26. The optimal response of the ideal analytical model (——) and the final response of the nonideal analytical model (o) for the two-section waveguide transformer.
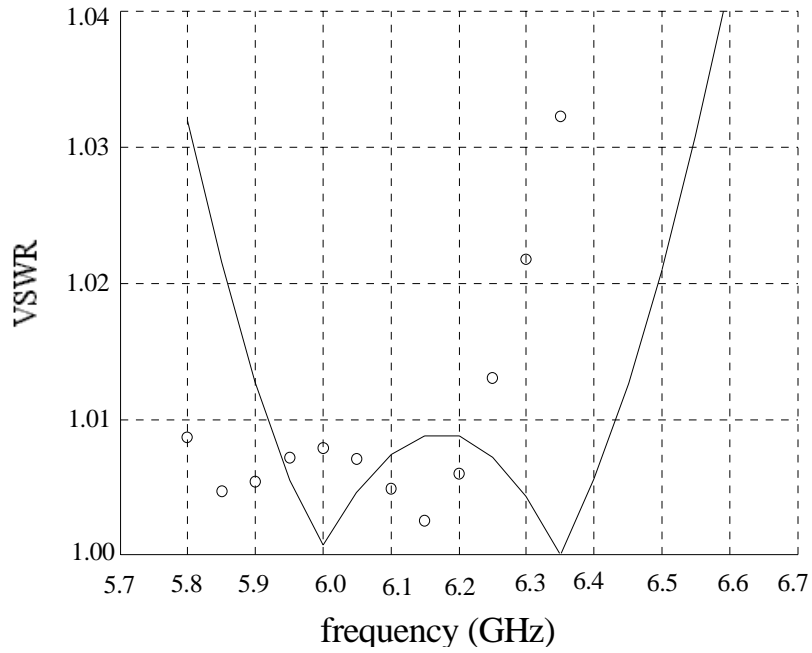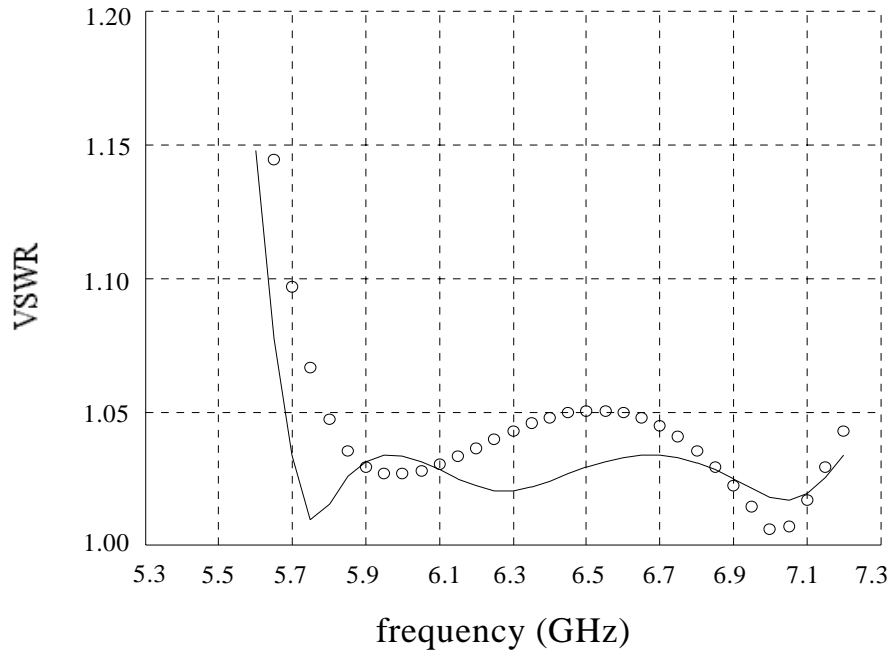
Fig. 27. The optimal response of the ideal analytical model (—) and the response of Maxwell Eminence (o) at the starting point for the two-section waveguide transformer.
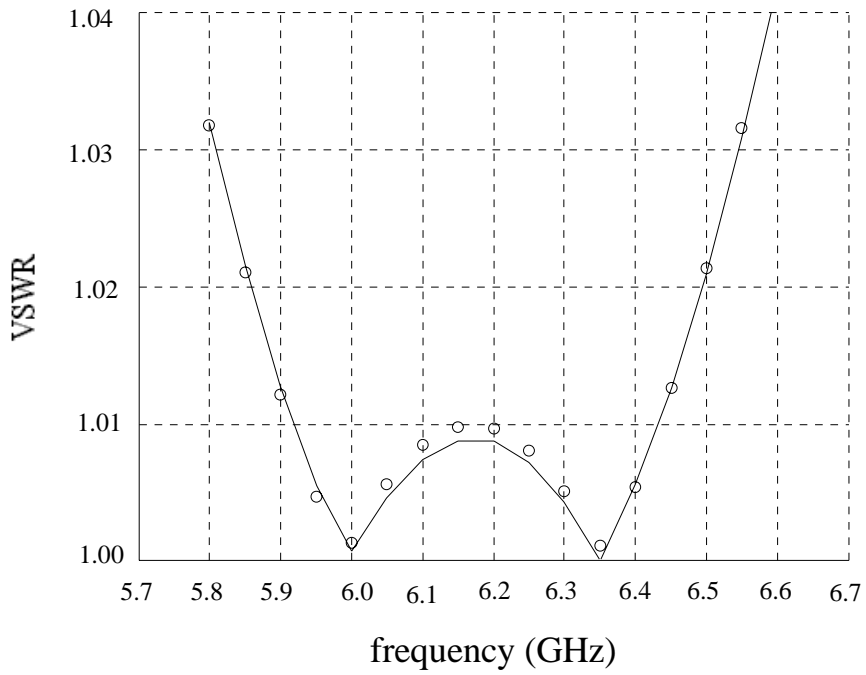
Fig. 28. The optimal response of the ideal analytical model (—) and the final Maxwell Eminence response (o) for the two-section waveguide transformer.

Fig. 29. The optimal response of the ideal analytical model (—) and the response of the nonideal analytical model (o) at the starting point for the three-section waveguide transformer.

Fig. 30. The optimal response of the ideal analytical model (—) and the final response of the nonideal analytical model (o) for the three-section waveguide transformer.

Fig. 31. The optimal response of the ideal analytical model (—) and the response of Maxwell Eminence (o) at the starting point for the three-section waveguide transformer.
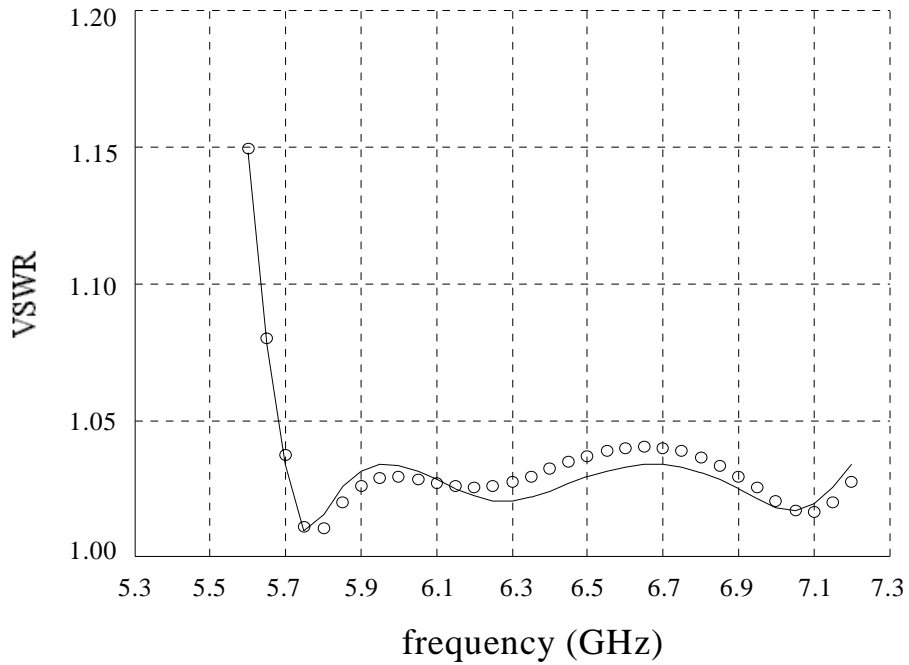

Fig. 32. The optimal response of the ideal analytical model (—) and the final Maxwell Eminence response (o) for the three-section waveguide transformer.
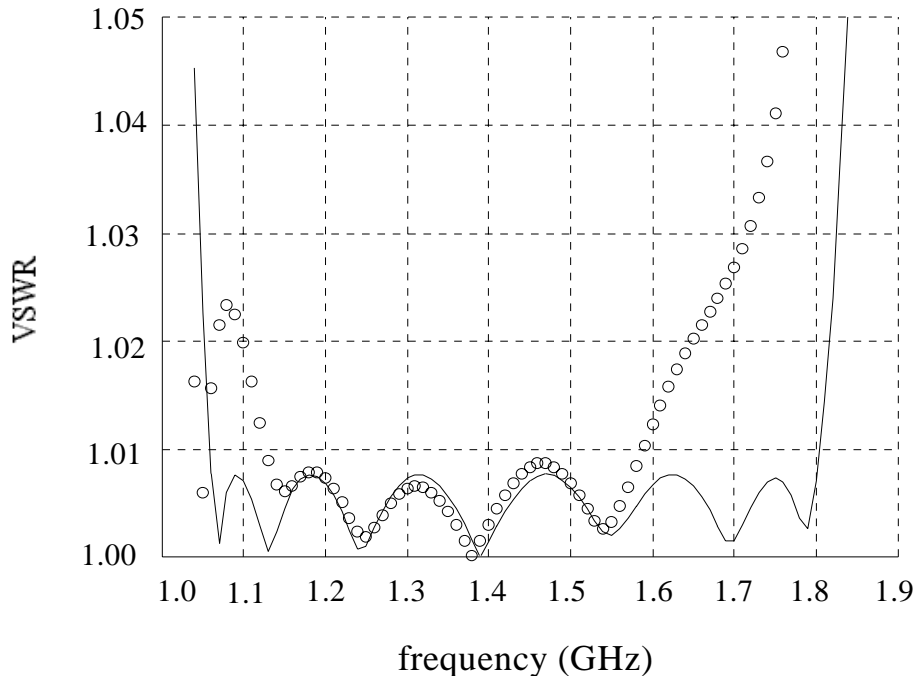
Fig. 33. The optimal ideal analytical model response (—) and the response of the nonideal analytical model (o) at the starting point for the seven-section waveguide transformer.
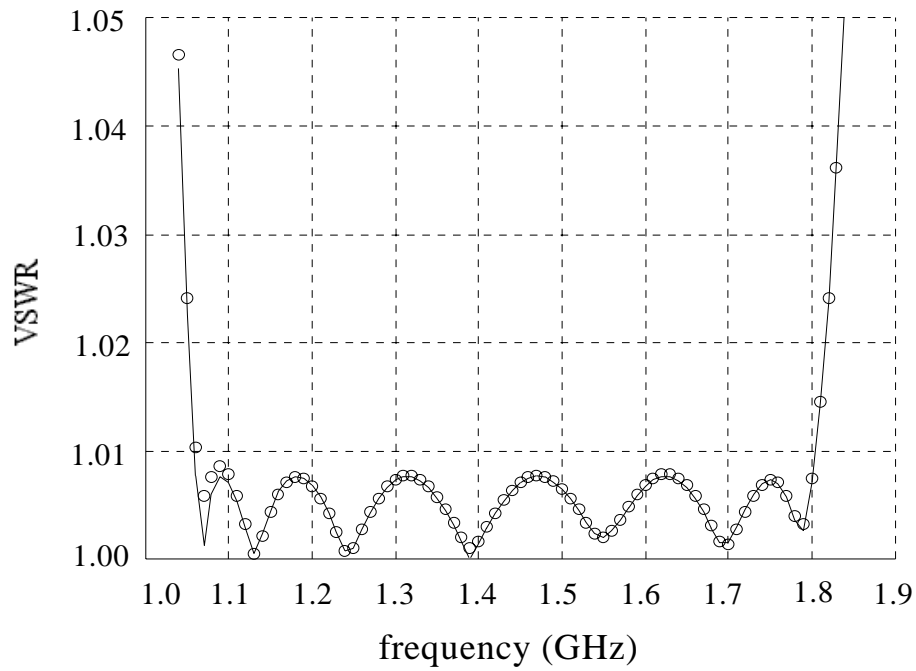

Fig. 34. The optimal response of the ideal analytical model (—) and the final response of the nonideal analytical model (o) for the seven-section waveguide transformer.
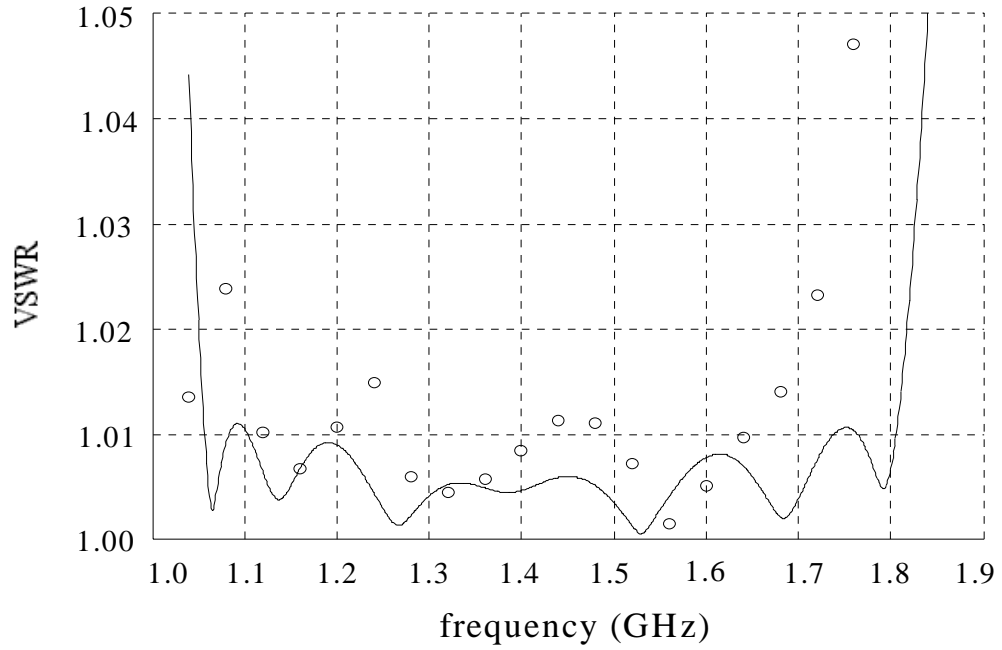
43

Fig. 35. The optimal response of the ideal analytical model (—) and the response of Maxwell Eminence (o) at the starting point for the seven-section waveguide transformer.
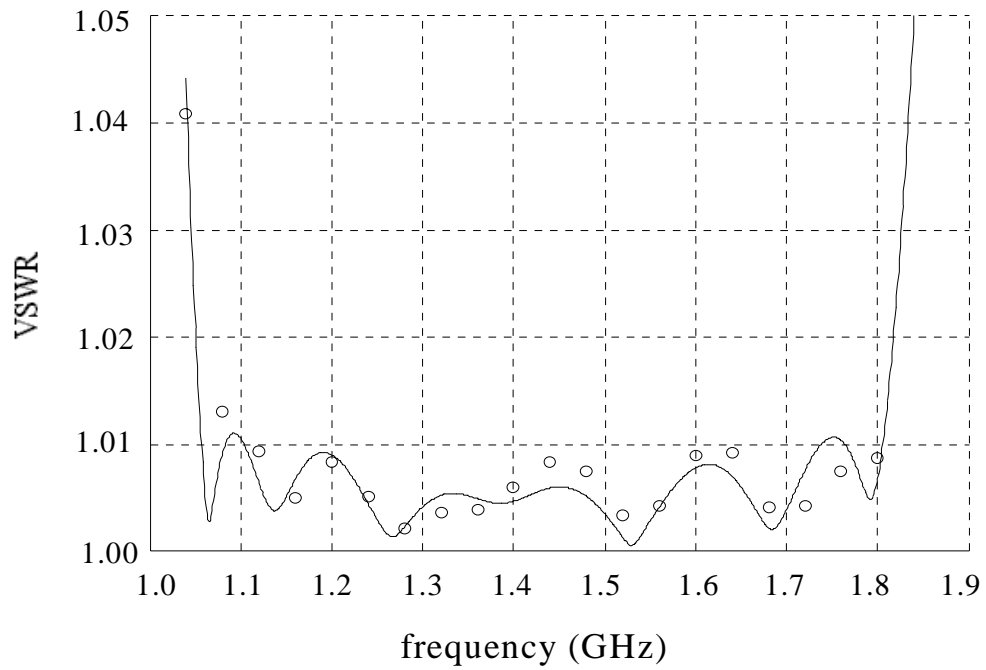

Fig. 36. The optimal response of the ideal analytical model (—) and the final Maxwell Eminence response (o) for the seven-section waveguide transformer.
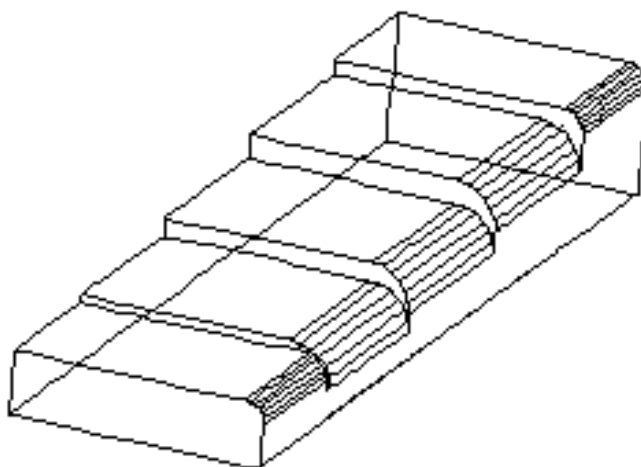
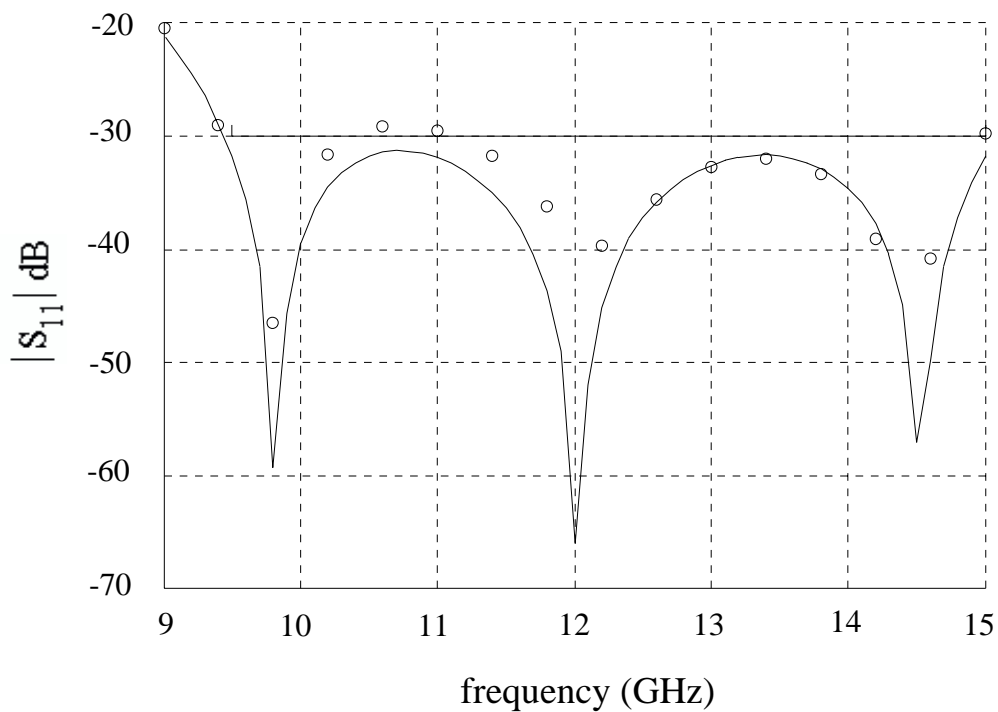Fig. 37. The simulated part of the three-section waveguide transformer with rounded corners [13].

Fig. 38. The optimal response of the ideal analytical model (——) and the response of HP HFSS (o) at the starting point for the three-section waveguide transformer with rounded corners.
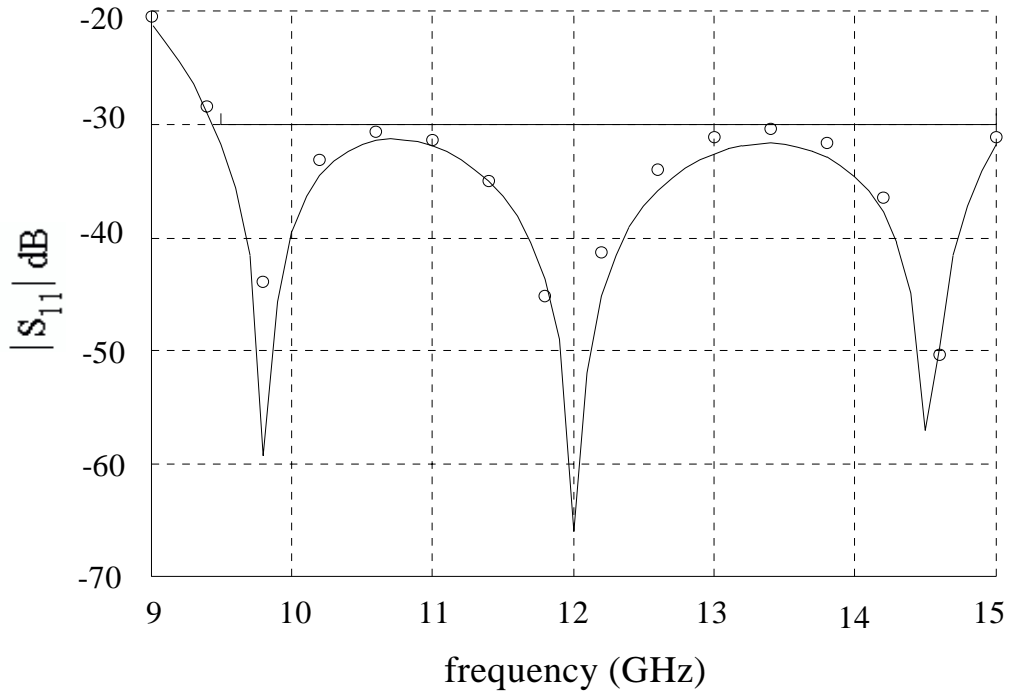
Fig. 39. The optimal response of the ideal analytical model (——) and the final HP HFSS response (o) for the three-section waveguide transformer with rounded corners.

Fig. 40. Monte Carlo analysis for the three-section waveguide transformer with rounded corners assuming 1% uniformly distributed parameters.
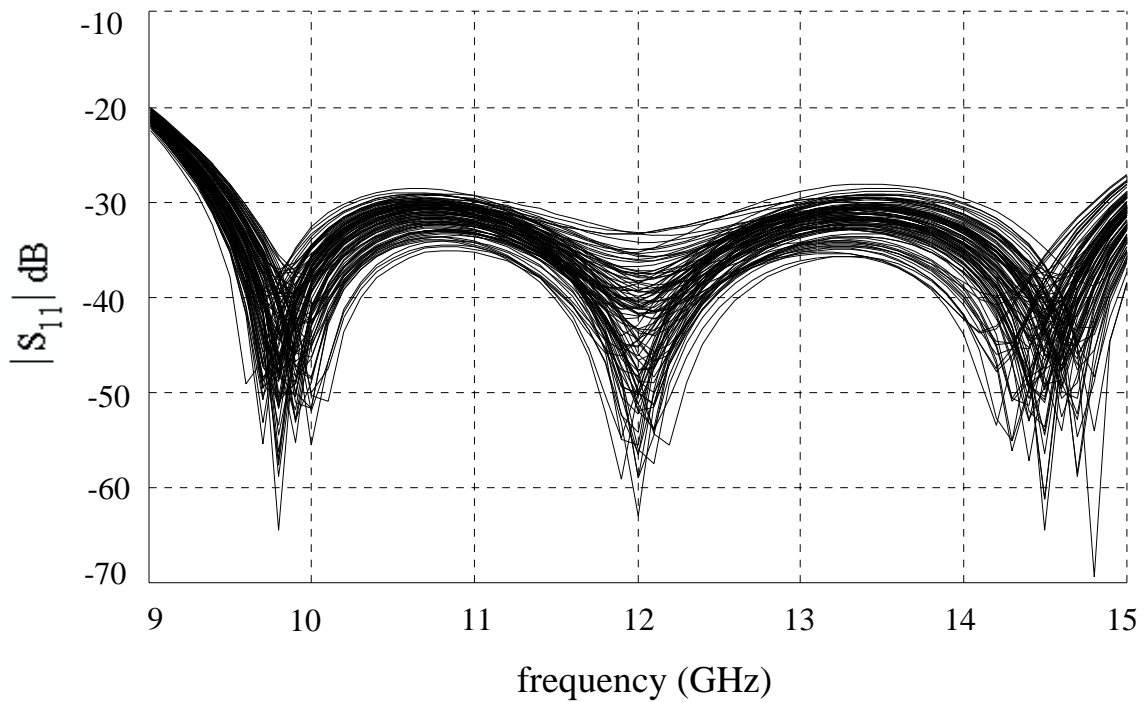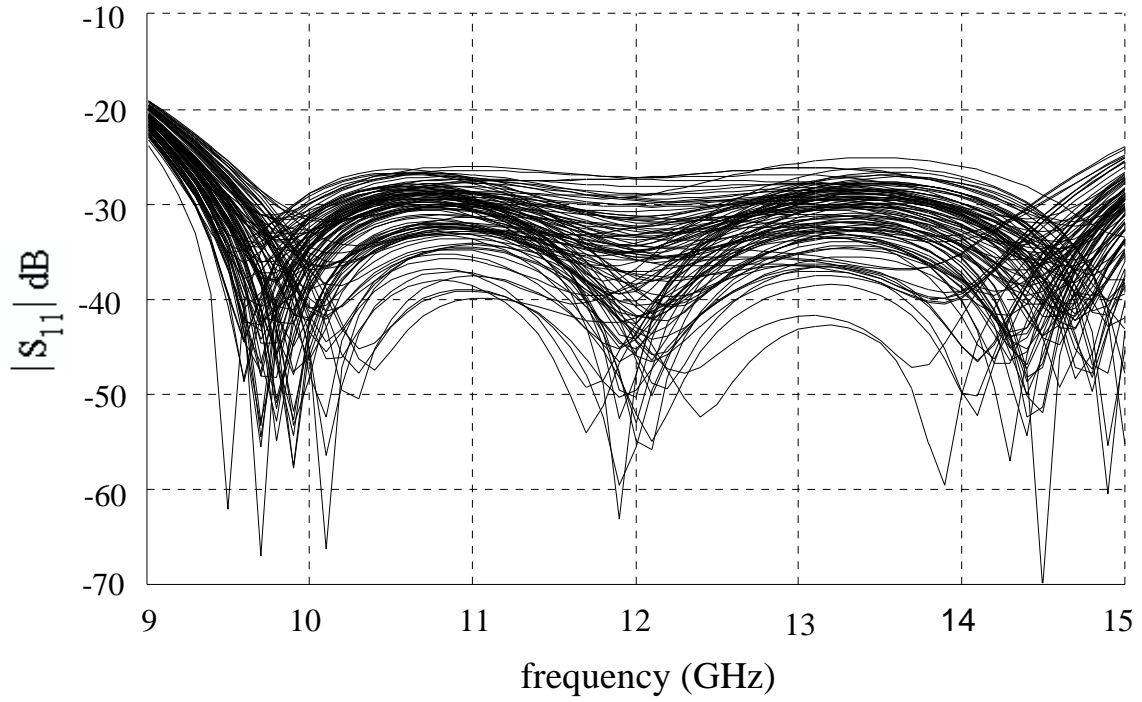
Fig. 41. Monte Carlo analysis for the three-section waveguide transformer with rounded corners assuming 2% uniformly distributed parameters.
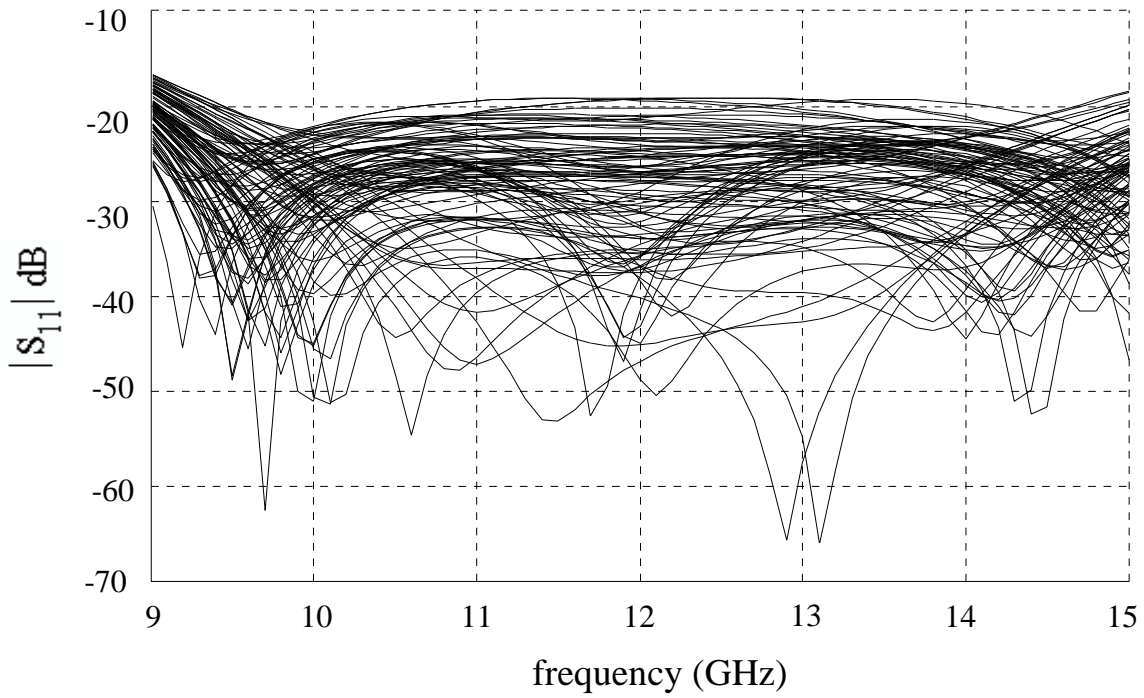

Fig. 42. Monte Carlo analysis for the three-section waveguide transformer with rounded corners assuming 5% uniformly distributed parameters.

APPENDIX A

! The OSA90/hope input file used for generating the fine model responses

```
Model
#include "wg7_osa/wg7.inc";
   Xem[14]=  ;                   ! fine model parameters are pasted in here
   Bos_opt[7] = [ 7.86732 6.61888 4.6854 2.91987 1.81412  1.27658  1.06847];
   Los_opt[7] = [ 7.10588 7.12201 7.1176 7.12331 7.12815  7.12154  7.12945];
   Xos_opt[14] = [Bos_opt Los_opt];
   ICONS = 0;
   ideal: 0;
   M: 7;
   M2 = M + 2;
   A[M2] = 16.51;
   B1[M2] = [8.255 Bos_opt 1.016];
   L1[M2] = [0 Los_opt 0];
   Datapipe: SIMD FILE="simwgd"
                  N_INPUT=(3 * M2 + 4)
                  INPUT=(M, A, B1, L1, ICONS, ideal, FREQ)
                  N_OUTPUT=1  OUTPUT=(VSWR_ideal); ! A Call to the coarse model
   WG7_H_1= 0.5*Xem[1];
   WG7_H_2= 0.5*Xem[2];
   WG7_H_3= 0.5*Xem[3];
   WG7_H_4= 0.5*Xem[4];
   WG7_H_5= 0.5*Xem[5];
   WG7_H_6= 0.5*Xem[6];
   WG7_H_7= 0.5*Xem[7];
   WG7_L_1= Xem[8];
   WG7_L_2= Xem[9];
   WG7_L_3= Xem[10];
   WG7_L_4= Xem[11];
   WG7_L_5= Xem[12];
   WG7_L_6= Xem[13];
   WG7_L_7= Xem[14];
   WG7  1 2 0  model=0
      H_1=(WG7_H_1 * 1cm)  H_2=(WG7_H_2 * 1cm)
      H_3=(WG7_H_3 * 1cm)  H_4=(WG7_H_4 * 1cm)
      H_5=(WG7_H_5 * 1cm)  H_6=(WG7_H_6 * 1cm)
      H_7=(WG7_H_7 * 1cm)  L_1=(WG7_L_1 * 1cm)
      L_2=(WG7_L_2 * 1cm)   L_3=(WG7_L_3 * 1cm)
      L_4=(WG7_L_4 * 1cm)   L_5=(WG7_L_5 * 1cm)
      L_6=(WG7_L_6 * 1cm)   L_7=(WG7_L_7 * 1cm); ! fine model parameter settings
   PORTS 1 0 2 0;
   CIRCUIT;
VSWR_non_ideal=(1+MS11)/(1-Ms11);
end
Sweep
   AC: FREQ: from 1.04GHz to 1.84GHz step=0.04GHz Vswr_non_ideal VSWR_ideal
      {XSWEEP title="VSWR and Spec" X=FREQ Xmin=1.0 Xmax=1.9 Nxticks=9
Y=Vswr_non_ideal.white.circle&VSWR_ideal.white
       Ymin=1.0 Ymax=1.05 Nyticks=5};
end
report
  $%12.9f$ R= [${ $VSWR_non_ideal$ }$ ]  ! The fine model response is saved using the
report feature
end
```

```
! The parameter extraction file used for multiplt parameter extraction
! for the seven section waveguide transformer

Model
    ICONS = 0;     ! This is the coarse model block
    ideal: 0;      ! It simulates the coarse model point given by the vector Xos
    M1: 7;
    M2 = M1 + 2;
    Bos[7] = [ Xos[1] Xos[2] Xos[3]  Xos[4]  Xos[5]  Xos[6]  Xos[7]];
    Los[7] = [ Xos[8] Xos[9] Xos[10] Xos[11] Xos[12] Xos[13] Xos[14]];
    A[M2] = 16.51;
    B1[M2] = [8.255 Bos 1.016];
    L1[M2] = [0 Los 0];
    Datapipe: SIMD FILE="simwgd"
                    N_INPUT=(3 * M2 + 4)
                    INPUT=(M1, A, B1, L1, ICONS, ideal, FREQ)
                    N_OUTPUT=1  OUTPUT=(VSWR_ideal);
End
expression
    i:1;
    n=14;
    m=21;
    N_Points=1 ;
    Kx: ((freq-1.04)/0.04)+1;
    j=nint(Kx);
    Bos_opt[7] = [ 7.86732 6.61888 4.6854 2.91987 1.81412 1.27658 1.06847];
    Los_opt[7] = [ 7.10588 7.12201 7.1176 7.12331 7.12815 7.12154 7.12945];
    Xos_opt[14] = [Bos_opt Los_opt];
    Xos_Matrix[1,n]=[ ?7.86793? ?6.61983? ?4.68604? ?2.92004? ?1.81394? ?1.27625?
                      ?1.06831? ?7.10616? ?7.12059? ?7.11628? ?7.12305? ?7.12756?
                      ?7.1196? ?7.12973? ];
    X_fine_Matrix[(n+1),n]=  ;    ! Paste the matrix of fine model points in here
    X_fine_Responses[(n+1),m]= ; ! Paste the matrix of fine model responses in here
    B[n,n]=  ;                    ! Paste the current B matrix in here
    X_fine[1:n]=row(X_fine_Matrix,i);
    X_fine_1[1:n]=row(X_fine_Matrix,1);
    X_coarse1[1:n]=row(Xos_Matrix,1);
    X_fine_Difference[1:n]=X_fine-X_fine_1;
    X_coarse_Difference[1:n]=product(B,X_fine_Difference);
    Xos[1:n]=X_coarse_Difference+X_coarse1;
end
specification
    i: from 1 to N_points step 1
            freq:  from 1.04 to 1.84 step=0.04
                        VSWR_ideal=X_fine_Responses[i,j];
end
sweep
   freq:  from 1.04 to 1.84 step=0.04
                    VSWR_ideal X_fine_Responses[1,j] {Xsweep Y=VSWR_ideal.white&
                    X_fine_Responses[1,j].white.circle Ymin=1 Ymax=1.05 Nyticks=5
xmin=1.0 xmax=1.9 Nxticks=9} ;
end
Control
    Optimizer=Huber;
    N_iterations=99;
    Huber_threshold=0.01;
    accuracy=1.0e-6;
    two_sided_jacobian;
end
report
 $%12.9f$ P = [ $ Xos_matrix[1,1]$
         $ Xos_matrix[1,2]$
         $Xos_matrix[1,3]$
         $Xos_matrix[1,4]$
```

```
        $Xos_matrix[1,5]$
        $Xos_matrix[1,6]$
        $Xos_matrix[1,7]$
        $Xos_matrix[1,8]$
        $Xos_matrix[1,9]$
        $Xos_matrix[1,10]$
        $Xos_matrix[1,11]$
        $Xos_matrix[1,12]$
        $Xos_matrix[1,13]$
        $Xos_matrix[1,14]$]
end
```